To
Dr. Kiefer, editor of *Climate of the Past*

Dr. Claudia Ehlert
Max Planck Research Group for Marine Isotope Geochemistry, Institute for Chemistry and Biology of the Marine Environment (ICBM)
University of Oldenburg
Carl-von-Ossietzky-Str. 9-11
D-26129 Oldenburg
Germany

Phone.: +49 (0)441 798 3345
Fax: +49 (0)441 798 3345
E-mail: cehlert@mpi-bremen.de

Oldenburg, 17 November 2014

Dear Dr. Kiefer,

we just have electronically submitted the revised manuscript for publication in *Climate of the Past* (#cp-2014-97) entitled "Nutrient Utilisation and Weathering Inputs in the Peruvian Upwelling Region Since the Little Ice Age" authored by C. Ehlert (corresponding author), P. Grasse, D. Gutiérrez, R. Salvatteci and M. Frank.
Again, we would like to thank here the reviewers for their constructive reviews and positive recommendations, which we took into account in preparing the revised manuscript and which we reply to in detail below. We would, however, like to point out that the changes made do not challenge any of the main conclusions of the manuscript.

Reply to Referee #1
In this manuscript, the authors present sediment Nd and Sr isotopes, biogenic silica%, organic nitrogen% and the isotopic composition of biogenic Si and N between 1300 and 2000 AD along the Peruvian coast. They found marked environmental changes between the little ice age (LIA) and recent times with higher riverine input and low productivity during the LIA due to "El Nino" like conditions. Furthermore, the author interpret the parallel increase between d30Si and d15N during the transition period as indicating that nutrient relative utilisation is the main process controlling n isotopic composition while denitrification has a relatively marginal influence on the isotopic signal. The author s are using a neat set of proxies to reconstruct past changes in climate and productivity in the study area. The Nd and Sr isotope data are quite compelling. Therefore I would support publication of this paper in Climate of the Past.
However, I have issues with the interpretation of the d15N and d30Si data and especially the conclusion that d15N responds mostly to changes in utilisation rather than denitrification. Therefore, the authors need to address this before I can fully support publication. First, the authors describe in both cores M771-470 and B0405-6 an increase in d30Si just after the LIA. If you take into account the error bars, only a couple of points in total fall below or above the others. To me the trend is not as marked as the authors describe it. Therefore I would argue that there is at most a 0.2 permil (from 0.7 to 0.9 permil) increase between the LIA and the rest of the record

(which is as much as the error bars) and would suggest only a modest increase in silicic acid utilisation. If you use a Raleigh fractionation model you would get something like 12% increase in utilisation.

Both cores show, as described and discussed in the manuscript, similar average $\delta^{30}Si_{bSiO2}$ values of +0.73‰ (B0405-6) and +0.85‰ (M771-470) during the LIA (see Fig. 2 of the manuscript). These are followed by a drop to +0.6‰ at the very end of the LIA and a subsequent rapid increase to +1.2‰ during the transitional period. Thereafter a decrease back to lower values near +0.9‰, similar to the LIA, in the most recent samples occurred, which is in full agreement with surface sediment samples from the area (see Fig. 4 in the manuscript and Ehlert et al., 2012). This corresponds to an overall change in $\delta^{30}Si_{bSiO2}$ of 0.6‰, and is therefore significantly higher than the uncertainties of the measurements.

In addition, this range in $\delta^{30}Si_{bSiO2}$ is essentially the same as the entire range measured in surface sediments along the Peruvian shelf region, which reflects silicic acid utilisation rates between 50 and 90% from the available pool (Ehlert et al., 2012). The maximum 0.6‰ difference in both records therefore corresponds to a change in utilisation between ~35% before the end of the LIA and 85% during the transition period, corresponding to an increase by 50% i (see Fig. 5a in the manuscript). Given that these calculations are based on few data points we decided to use average values for the different time periods which decreases the maximum $\delta^{30}Si_{bSiO2}$ range, but the pronounced change in utilisation between the LIA and transition period remains significant.

At the same time, the opal % records and valve accumulation rates show a 2 to 3 fold increase depending on the core site. Figure 5 shows a much greater gradient in utilisation between the time slices considered but I believe this is because for the transition period for instance only one d30Si data point is taken into account.

Actually, the values are exactly the ones described above, which in the case of the transition period varies between +1‰ and +1.2‰, as plotted in Fig. 5. The values are defined by a total of 4 data points, 2 for each core.

I am also wondering whether the authors took into account the fairly low modern d30Si values from core b0405-6 (to me indistinguishable from the LIA values) when they plotted the period-specific relative utilisations on the fractionation curves (Fig 5).

This is correct and it is in fact one of the most important points of our entire manuscript (!) that the $\delta^{30}Si_{bSiO2}$ during the LIA and in modern sediments show essentially the same values (and therefore the same silicic acid utilisation), but at the same time show significantly different $bSiO_2$ concentrations, which leads us to the conclusion that the total amount of dissolved nutrients (in partuicular silicic acid) must have been markedly different between the LIA and the present (see section 4.1.4 in the manuscript).

Yes, all measured $\delta^{30}Si_{bSiO2}$ values have been taken into account when calculating the mean $\delta^{30}Si_{bSiO2}$ as well as $\delta^{15}N_{sed}$ values for the period-specific utilisation calculations (except for the oldest $\delta^{30}Si_{bSiO2}$ data point of core B0405-6,

because it is slightly older than the LIA according to the age model but shows essentially same value as the LIA-samples).

Now the d15N records show a much more defined trend with about 2 permil lower values during the LIA compared to modern. That's an increase of about 40% in N utilisation between the LIA and the modern (according to figure 5) if you believe denitrification had only a marginal impact on the d15N signal.

This translates into an increase in utilisation very similar to the one indicated by silicon isotopes (see comment above). The only difference is that the signal obtained from the $\delta^{15}N$ shows a one step increase from the LIA to modern, whereas the $\delta^{30}Si$ shows a (slight) decrease at the end of the LIA and after the transition period. This is discussed in detail in the text of the manuscript, e.g. in section 4.1.4.

The timing of change is very consistent between all core sites while it is not for the d30Si. Therefore, this casts doubt on the assertion that nitrate and silicic acid utilisation increased in parallel during the transition period in response to increased upwelling.

A difference in timing between the $\delta^{15}N$ and $\delta^{30}Si$ changes is not clearly resolvable based on the coarser resolution of our $\delta^{30}Si$ record (these $\delta^{30}Si$ values are much harder and more time consuming to produce) given that there is no data point for the earliest part of the transition period in core B0405-6, which in core M771-470 is clearly already marked by high $\delta^{30}Si$ values. So, the timing of the changes may well be exactly the same which led us to the interpretation that the changes were in both cases mainly caused by an increase in utilisation given the pronounced increase in diatom abundance, $\delta^{30}Si$ and N concentrations.

Now there is a theoretical problem as well: With increased upwelling, studies have overwhelmingly shown that nitrate utilisation should decrease due to the influx of a great quantity of nitrate to the surface (more nitrate is utilised by the blooming algae but even more is left behind unutilised, hence reducing the recorded relative utilisation (see early papers from Francois and Altabet)). The author of the present paper argue that increasing upwelling and biological production at the end of the LIA resulted in an increase in d15N and d30Si and that it shows that relative utilisation of both nutrients increased together. I have to disagree with this interpretation. To me d15N increased because of increased denitrification promoted by higher organic matter rain rate (higher oxidant demand at depth or in the sediment). D15N indeed increased more than d30Si because it is mostly responding to denitrification and not relative utilisation. The modest and spatially variable increase in d30Si after the LIA does not match the very clear, consistent 2 permil increase in d15n. To me that tells us that both proxies are governed by different processes. It is possible to imagine that Silicic acid was abundant at the sea surface due to increased run off and was also less utilised during the LIA because the conditions where unfavourable to the diatom community (stratification) but that during the transition period they became favourable and hence the diatoms where able to utilised a greater proportion of the available Si (diatom production more than doubled while Si utilisation increased only

slightly). I expect in the other hand that nitrate relative utilisation (which depends on diatoms and other planktonic producers) overall decreased or only slightly increased between the LIA and the modern period but the large d15N increase is mostly due to the kick off of denitrification.

We are thankful that the reviewer's comment gives us the possibility to highlight again our interpretation of the Si/N isotope records. We would like to point out here that we do not neglect the influence of NO_3^--loss processes on the preserved $\delta^{15}N_{sed}$ record, and we did not do so in the manuscript. In contrast, we mentioned at several points that both utilisation and NO_3^--loss processes played a role. However, we would like to emphazise in this manuscript that utilisation is an important factor that is often underestimated in the interpretations of the records, especially in a region like the EEP where studies have shown that the heavier N isotope signatures during NO_3^--loss processes are only preserved in the sediments under conditions of near-complete surface water utilisation of the nutrients (Mollier-Vogel et al., 2012). This, however, did not occur most of the time during the past ~600 years, as our $\delta^{30}Si_{opal}$ records document.

The patterns and changes in Si isotope composition of both cores presented in this manuscript are fully consistent with the record presented in Ehlert et al. (2013), where we demonstrated for the past ~20,000 years that periods of high biogenic opal deposition, i.e. high PP, consistently corresponded to periods with high utilisation of silicic acid/nutrients. In the records presented here biogenic opal concentrations, total amount of diatom valves, and total nitrogen concentrations all start to increase at the same time documenting that diatoms where the drivers of the increased PP at the end of the LIA and during the transition period. Additionally, higher biogenic opal deposition also corresponds to higher $\delta^{15}N$ values, i.e. higher nitrate utilisation.

The relative increase in $\delta^{15}N$ is NOT higher than the increase in $\delta^{30}Si$. When applying the utilisation models both show an approximately doubling in utilisation from the LIA to the transition period (see Fig. 5 in the manuscript). However, it is true that after the transition period, the calculated utilisation from the $\delta^{15}N$ is ~20% higher than from the $\delta^{30}Si$, which we interpret to be indicative of the influence of enhanced denitrification. To clarify that point in the manuscript we propose the following additional paragraph in section 4.1.4 (p.15, L. 453-464 in the revised manuscript):
"In the modern samples the $\delta^{30}Si_{opal}$ are characterised by a slight decrease after the transition period from mean value of +1.12‰ to +0.82‰, whereas the $\delta^{15}N_{sed}$ values remain at the same level around +7‰ (Fig. 2). This corresponds to a ~20% higher NO_3^- than $Si(OH)_4$ utilisation (Fig. 5). However, when assuming that diatoms are the dominating primary producers with a NO_3^-:$Si(OH)_4$ uptake ration of ~1, these 20% could be interpreted to reflect the increase in subsurface NO_3^--loss that is not observable during the LIA or the transition period. I.e. during the LIA and the transition period utilisation was the domniating process influencing the $\delta^{15}N_{sed}$ signal, whereas during modern times NO_3^--loss enhanced the signal. By combining the $\delta^{30}Si_{opal}$ and the $\delta^{15}N_{sed}$ records this "additional" signal can be quantified here: if only utilisation would play a role the expected $\delta^{15}N_{sed}$ signal would be ~+6‰ (corresponding to the measured ~+0.8‰ for $\delta^{30}Si_{opal}$, Fig. 5). The additional 1‰ $\delta^{15}N_{sed}$ must be due to NO_3^--loss."

I also note that the authors use a d15N-nitrate source signal of 4 permil (fig. 5) while today this signal is known to be much higher in this region due to intense denitrification. At least for the reconstruction of the modern nitrate relative utilisation a greater d15N source value should be used.

No, we used a source signature of +9‰ as described in the text (e.g., p.3373 L.15 of the discussion manuscript, p.14, L.431-432 in the revised manuscript) and also shown in the Figures (left scales in Fig. 5). This is the signature that has been measured in the present day Peruvian Undercurrent (Mollier-Vogel et al., 2012), which is the source water for the upwelling and therefore delivers the nutrients to the surface waters.

Minor comments: Line 12 p3360: "this fractionation process is mainly controlled by the availability of Si(OH)4: : :" I believe this is incorrect. I would rephrase this as follow: "Si isotopic fractionation is mainly controlled by the utilisation of silicic acid in the sea surface by the biota".

Yes, we have changed the sentence as suggested (see p.3, L81-82 in the revised manuscript).

Reply to Referee #2

I have reviewed Ehlert an co-authors' results on radiogenic sedimentary Nd and Sr isotopes, biogenic silica, total nitrogen and the isotopic composition of biogenic Si and bulk N between 1300 and 2000 AD from 2 new sedimentary archives off the Peruvian coast. The paper is well written and it could provide the community with a better understanding of the relationship between global climate and local oceanographic changes happening during the past 700 years and the LIA potential impacts on the eastern South Pacific. I think that this would be very relevant for future predictions on how this critical part of the ocean for food supply will evolve as climate changes. The new data (radiogenic isotopes and silicon isotopes) definitely merits publication in Climate of the Past but I would suggest some major revisions to the way the authors have presented their dataset.

My main concern is the following: since a great deal of the data presented here has been already published elsewhere, (Gutiérrez et al 2006, 2009; Siffedine et al., 2008), and the true novelty comes from the Nd, Sr and Si isotopes, it would be more natural to focus the bulk of the publication on these variables and how they fit in a more global picture of changes associated with ocean circulation and climate change, specially at the critical period that they have highlighted following 1820-1870AD. Instead, it was very disappointing to see that in its present form, the paper presents a very long discussion on nutrient utilization, which is highly debatable.

In fact, only bSi, TN, diatom accumulation rates and the $\delta^{15}N_{sed}$ data of core B0405-6 have been published before and are compared to our new Si, Nd and Sr isotope data, as well as to the new bSi and TN concentration data of core M771-470. So the amount of new data in this manuscript is high and the novelty comes from the direct comparison of the different proxies, in particular of the Si and N isotope data.

The (long) discussion of nutrient utilisation, in particular the comparison between Si and N isotope data arises from the fact that we have to interpret especially the $\delta^{15}N_{sed}$ data in a way that differs from other open ocean and near costal sites (see review #1). This is one of the key and novel parts of the implications of our data, which correspondingly needs a thorough discussion.

We decided not to speculate about any global implications of the data but rather focused on comparison to other regional data sets in the eastern Pacific.

What can the authors say about the Nd signature of the 2 cores and changes associated with ENSO or SAM during this period? In my opinion, the paper's major strength and novelty should be set in linking the radiogenic isotope results (and silica isotopes) to climate and leave the nutrient utilization discussion as it is or shorten it up.

As described above, we wanted to focus in our manuscript on the comparison between our novel Si (and Nd, Sr) isotope data to existing records from the region, which we then put into a wider regional or global context of oceanic and atmospheric circulation changes. Our new data are consistent with these records and support and strengthen the interpretation of a change from predominant El Nino-like conditions during the LIA to La Nina-like conditions in the modern EEP. In addition, we show that centennial scale changes in the records presented in our study are caused by similar processes as changes on millenial and glacial-interglacial time scales.

We also see that both reviewers highlight the radiogenic isotope data as being interesting and useful but that the potential of discussion has not been fully exploited, which we try to improve in the revised version of the manuscript. We strengthened our argumentation by better linking the radiogenic and stable isotope data and by highlighting the comparison and agreement with existing interpretations in section 4.2 (see p.19, L.566-616 in the revised manuscript). We also changed the order of the paragraphs in section 4.1.5 to highlight the connenction to the following section 4.2 (without changing the content of section 4.1.5).

My second concern with the paper in its present form deals with the M771-470's age control during the critical transition period highlighted and discussed thoroughly in the paper. The core's age model beyond 1850AD was constructed by adopting the sedimentation rates of (not so) nearby core B0405-13. In this respect, it is worth noting that sedimentation rates at both sites appear to be very different. Just take the case of the sed. rate of M771-470 from 10 to 25 cm being as low as half of B0405-13's sed. Rate (0.9 vs 1.78 mm yr-1). Why should these 2 cores have a similar sed. rate in the past if recent sedimentation regimes are so different? I am not disregarding the age model proposed here, but I would like to see a much thorough justification of it.

It is notoriously difficult to obtain reliable age models for sediment cores from the shelf off Peru but in our case it was possible to make use of a lot of independent information to establish the chronology, which thus can be considered well-constrained. The major change in biogeochemical proxies at ~28 cm core depth in core M771-470 is considered a reliable and independent time marker, which has been found in many cores from the region and has been dated to 1820 ± 15 years AD

(Salvatteci et al., 2014b, and references therein), which agrees well with our estimated age based on ^{210}Pb dating. Before that, during the LIA, the Peruvian upwelling system was less productive all along the coast leading to much lower sedimentation rates. Both cores B0405-13 at ~12°S and B0405-6 at ~14°S show a sedimentation rate of 0.6mm/yr during the LIA, which we used for the age model of core M771-470.

After the LIA, productivity increased markedly. The ^{210}Pb dating gives an age of 214 years for the uppermost 25cm (with no indication of any hiatus), which results in an average sedimentation rate of ~1.2mm/yr, which compares well to the sedimentation rates of cores B0405-6 and -13, as well as other cores from the region. However, there is bioturbation in the uppermost 10cm of core M771-470 (=same ^{210}Pb age for 0-10cm depth), which is why we were only able to calculate sedimentation rates only for the depths 10-25cm, which resulted in 0.92mm/yr.

We decided to use a higher sedimentation rate of 1.5 mm/yr of core B0405-13 for our age model of the transition period because this core reveals comparable sediment properties, was recovered from a similar water depth, etc. The increase in PP parameters (diatom valve amount, $bSiO_2$ and TN concentration) is a typical pattern of the transition period that was also found in other records (e.g., Salvatteci et al., 2014a,b). In addition, the increase in porosity in core M771-470, similar to the change in density in cores B0405-6 and -13 and multiple others (9 in total, Salvatteci et al., 2014b), is a suitable marker for the transition period. These considerations lead us to the conclusion, that the adaptation of the sedimentation rate of core B0405-13 is appropriate.

Another minor comment would be to ask the authors to refrain from asserting certain climate connection as certain since this is all very speculative yet. For example, in the abstract the authors write "...These patterns were caused by permanent El Niño like conditions characterized..." (emphasis added). This is too strong phrasing that implies complete certainty. I would advice the authors to try to keep a more speculative language when asserting hypothetical causalities that are going to be surely subject of confirmation (or rejection) by future work.

The text of the Abstract was changed as suggested (see p.2, L.29 in the revised manuscript).

However, we would also like to state here that e.g. the characterization of El Nino-like conditions during the LIA in the Tropical Pacific has been shown by several studies using different proxies, to which our work agrees well. Thus the causal relationships presented in the Abstract and throughout the text are not as hypothetical as the reviewer suggests.

We hope that we could answer all points raised by the reviewers and we hope that our manuscript will now be suitable for publication in *Climate of the Past.* All co-authors have seen the manuscript and agree to its re-submission.

With best regards,

Claudia Ehlert

Nutrient Utilisation and Weathering Inputs in the Peruvian Upwelling Region Since the Little Ice Age

C. Ehlert[1,*], P. Grasse[1], D. Gutiérrez[2], R. Salvatteci[2,3] and M. Frank[1]

[1] GEOMAR Helmholtz Centre for Ocean Research Kiel, Germany

[2] Instituto del Mar del Perú (IMARPE), Dirección de Investigaciones Oceanográficas, Callao, Peru

[3] Institute of Geoscience, Department of Geology, Kiel University, Ludewig-Meyn-Str. 10 D-24118 Kiel, Germany

[*] now at: Max Planck Research Group for Marine Isotope Geochemistry, Institute for Chemistry and Biology of the Marine Environment (ICBM), University of Oldenburg

Correspondence to: C. Ehlert (cehlert@mpi-bremen.de)

Keywords:

stable silicon isotopes, stable nitrogen isotopes, primary productivity, river input, eolian input, material transport, Little Ice Age, nutrient utilisation

Abstract

For this study two sediment cores from the Peruvian shelf covering the time period between the Little Ice Age (LIA) and present were examined for changes in productivity (biogenic opal concentrations (bSi)), nutrient utilisation (stable isotope compositions of silicon ($\delta^{30}Si_{opal}$) and nitrogen ($\delta^{15}N_{sed}$)), as well as in ocean circulation and material transport (authigenic and detrital radiogenic neodymium (ε_{Nd}) and strontium ($^{87}Sr/^{86}Sr$) isotopes).

For the LIA the proxies recorded weak primary productivity and nutrient utilisation reflected by low average bSi concentrations of ~10%, $\delta^{15}N_{sed}$ values of ~5‰ and intermediate $\delta^{30}Si_{opal}$ values of ~0.9‰. At the same time the radiogenic isotope composition of the detrital sediment

fraction indicates dominant local riverine input of lithogenic material due to higher rainfall in the Andean hinterland. These patterns were most likely caused by permanent El Niño-like conditions characterized by a deeper nutricline, weak upwelling and low nutrient supply. At the end of the LIA, $\delta^{30}Si_{opal}$ dropped to low values of +0.6‰ and opal productivity reached its minimum of the past 650 years. During the following transitional period of time the intensity of upwelling, nutrient supply and productivity increased abruptly as marked by the highest bSi contents of up to 38%, by $\delta^{15}N_{sed}$ of up to ~7‰, and by the highest degree of silicate utilisation with $\delta^{30}Si_{opal}$ reaching values of +1.1‰. At the same time detrital ε_{Nd} and $^{87}Sr/^{86}Sr$ signatures documented increased wind strength and supply of dust to the shelf due to drier conditions. Since about 1870, productivity has been high but nutrient utilisation has remained at levels similar to the LIA indicating significantly increased nutrient availability.

Comparison between the $\delta^{30}Si_{opal}$ and $\delta^{15}N_{sed}$ signatures suggests that during the past 650 years the $\delta^{15}N_{sed}$ signature in the Peruvian Upwelling area has to a large extent been controlled by surface water utilisation and not, as previously assumed, by subsurface nitrogen loss processes in the water column, which only had a significant influence during modern times (i.e. since ~1870 AD).

1 Introduction

Global climate of the late Holocene was disrupted by major anomalies, the most recent of which being the Little Ice Age (LIA) between ca. 1400 and 1850 AD (Lamb, 1965; Grove, 2001). During that time a weakening of the Walker circulation (Conroy et al., 2008), reduced influence of the South Pacific subtropical high (SPSH) along the Peruvian margin (Sifeddine et al., 2008; Gutiérrez et al., 2009; Salvatteci et al., 2014a), and a southward shift of the mean position of the Intertropical Convergence Zone (ITCZ) and the associated precipitation belt compared to today (Sachs et al., 2009) caused pronounced changes in rainfall patterns in the tropics. El Niño-like warmer conditions in the Eastern South Pacific were accompanied by an intensified South American summer monsoon (Bird et al., 2011) resulting in ~10% higher precipitation in northeast Peru (~5°S; Rabatel et al., 2008) and up to 20-30% higher precipitation in the Bolivian Andes (~16°S; Reuter et al., 2009). On the one hand this caused growth and extension of the Andean glaciers (Vuille et al., 2008) and on the other it enabled human settlements in the presently hyperarid southern Peruvian Andes (Unkel et al., 2007). In

the upwelling areas off Peru and the western South American shelf regions the main consequence of these climatic conditions during the LIA was a deepening of the nutricline and a strongly diminished biological productivity (Vargas et al., 2007; Sifeddine et al., 2008; Valdés et al., 2008; Gutiérrez et al., 2009).

Sediment cores from the Peruvian shelf covering the period of time from the LIA until present indicate that the marine realm was characterised by an abrupt biogeochemical regime shift towards modern conditions at the end of the LIA due to the northward movement of the ITCZ and an expansion of the SPSH. While low productivity and a more oxygenated water column prevailed during the LIA, markedly increased biological productivity and pronounced oxygen depletion over wide areas of the shelf have characterised the system since the end of the LIA (Vargas et al., 2007; Sifeddine et al., 2008; Gutiérrez et al., 2009, Salvatteci et al., 2014a).

In this study the stable silicon isotope composition of sedimentary diatoms ($\delta^{30}Si_{opal}$) covering the period of time from the LIA to the present is analysed. The main goal is the reconstruction of the factors controlling the dynamics of nutrient cycling together with oxygen in the Peruvian upwelling, in particular a comparison between the $\delta^{30}Si_{opal}$ and the stable nitrogen isotope composition ($\delta^{15}N_{sed}$) of sedimentary organic matter. Both $\delta^{30}Si_{opal}$ and $\delta^{15}N_{sed}$ provide information about utilisation of silicic acid ($Si(OH)_4$) and nitrate (NO_3^-) during primary productivity, e.g. during the formation of diatom frustules and associated organic matter, respectively (Altabet and Francois, 1994; De La Rocha et al., 1997). Diatoms preferentially incorporate the lighter isotopes from the dissolved $Si(OH)_4$ and NO_3^- pools leaving the residual dissolved nutrients enriched in the heavier isotopes (Wada and Hattori, 1978; Altabet et al., 1991; De La Rocha et al., 1997). Si isotope fractionation is mainly controlled by the utilisation of $Si(OH)_4$ in surface waters by biota (diatoms) (e.g., De La Rocha et al., 1998; Brzezinski et al., 2002; Egan et al., 2012). The $\delta^{15}N$ of NO_3^- is partly controlled by NO_3^- utilisation of marine organisms but is also affected by N-loss processes in the water column (denitrification, anammox) (Codispoti et al., 2001; Dalsgaard et al., 2003) resulting in a marked enrichment of the upwelling source waters in the heavier $^{15}NO_3^-$ (Liu and Kaplan, 1989; Lam et al., 2009; given that it is currently not possible to distinguish between different N-loss processes from the sediments we will use the term denitrification for simplicity). Consequently, sedimentary $\delta^{15}N_{sed}$ records from areas dominated by oxygen-depleted waters such as the shelf region off Peru are usually interpreted to directly reflect changes in the intensity of subsurface NO_3^- loss and the extent and strength of oxygen

mm mpi 11/3/14 9:29 AM
Deleted: For the $\delta^{30}Si_{opal}$ this fractionation process is mainly controlled by the availability of $Si(OH)_4$ in surface waters

depletion (e.g., De Pol-Holz et al., 2007, 2009; Agnihotri et al., 2008; Gutiérrez et al., 2009) whereas the effect of NO_3^- utilisation on the preserved $\delta^{15}N_{sed}$ is often neglected. Comparison of both isotope systems can therefore provide information about the degree of utilisation of NO_3^- and $Si(OH)_4$ versus the influence of NO_3^- loss processes. Increasing nutrient utilisation should result in a consistent increase in both $\delta^{30}Si_{opal}$ and $\delta^{15}N_{sed}$. In contrast, a change in NO_3^- reduction due to varying oxygen depletion in the water column would affect only the $\delta^{15}N_{sed}$ leaving the $\delta^{30}Si_{opal}$ unaffected.

The main forces driving surface productivity and subsurface oxygenation off Peru at centennial time scales during the past two millennia have been changes in the strength of the Walker circulation and in the expansion/contraction of the SPSH (Gutierrez et al., 2009; Salvatteci et al., 2014a). Therefore, the radiogenic isotope compositions of neodymium (ε_{Nd}) and strontium ($^{87}Sr/^{86}Sr$) of the authigenic ferromanganese (Fe-Mn) oxyhydroxide coatings of the sedimentary particles, which are expected to record the radiogenic isotope compositions of past bottom waters, as well as of the detrital fraction of the sediment were examined. These proxy data provide information about changes of (surface ocean) circulation and of transport processes, provenance of the sediments, and input mechanisms of terrigenous material as a function of changes in precipitation on land during the transition from wetter LIA-conditions to drier modern conditions. Weathering of continental source rocks delivers lithogenic particles of different origin and age to the shelf, which have distinct radiogenic isotope signatures ($\varepsilon_{Nd\ detritus}$, $^{87}Sr/^{86}Sr_{detritus}$) that can be used to trace their source areas (Goldstein et al., 1984). Central Peruvian Andean rocks have more radiogenic ε_{Nd} signatures whereas southern Peruvian rocks are characterised by less radiogenic ε_{Nd} signatures (Sarbas and Nohl, 2009), which is also reflected in the sediments along the shelf (Ehlert et al., 2013). Changes in detrital material input and transport pathways are generally closely related to climatic changes causing variations in the supply from the respective source areas (e.g. Grousset et al., 1988). It should therefore be possible to detect the transition from wetter LIA-conditions with higher local input from central Peru via rivers due to higher precipitation rates towards the drier presently prevailing conditions with an increased influence of eolian material transport from further south in the Atacama desert (Molina-Cruz, 1977) and deposition along the shelf after the LIA.

2 Material and Methods

2.1 Core Locations and Age Models

For the reconstruction of surface water $Si(OH)_4$ utilisation and terrestrial material input and transport for the period of time between the LIA and present two sediment cores with high sedimentation rates were analysed. Box core B0405-6 was recovered from the upper continental slope off Pisco at 14°07.9' S, 76°30.1' W in a water depth of 299 m with the Peruvian R/V José Olaya Balandra in 2004 (Fig. 1) (Gutiérrez et al., 2006). The age model was previously published by Gutiérrez et al. (2009) and is based on downcore profiling of the activities of ^{241}Am, excess ^{210}Pb, and on radiocarbon ages obtained from bulk sedimentary organic carbon, which document that the core covers the past ~650 years. The second core, multicorer M771-470, was taken at 11° S, 77°56.6' W in 145 m water depth during cruise M77/1 with the German R/V Meteor in 2008 (Fig. 1). The age model was obtained by measuring excess ^{210}Pb activities and modeling of the resulting profiles as described by Meysman et al. (2005) (for details see Supplement). Ages prior to ~1850 AD were inferred using sedimentation rates from nearby core B0405-13 (Gutiérrez et al., 2009; Salvatteci et al., 2014b).

2.2 Methods

2.2.1 Biogenic Opal and Silicon Isotope Analyses

The biogenic opal (bSi) contents in both cores were measured following the sequential leaching techniques described by DeMaster (1981) and Müller and Schneider (1993). Si isotope analyses were performed on the 11-32µm diatom-fraction that was extracted from the sediment applying the procedures described by Morley et al. (2004).

Approximately 300 mg of sediment were treated with 30% H_2O_2 and 35% HCl to remove organic matter and carbonate. Afterwards the sediment was wet-sieved to separate the 11-32 µm fraction. In a third step a heavy-liquid solution (sodium-polytungstate, 2.1-2.2 g/mL) was applied in several steps to separate diatoms from the detrital lithogenic silicate material. All samples were screened under the microscope to verify their purity with respect to the detrital (clay) fraction.

The diatom samples were then transferred into Teflon vials and dissolved in 1 mL 0.1 M

NaOH and diluted with MQ water according to Reynolds et al. (2008). More details are provided in Ehlert et al. (2012). Si concentrations of the dissolved diatom samples were measured colorimetrically using a photospectrometer (Hansen and Koroleff, 1999). Chromatographic separation and purification of the Si was achieved with 1mL pre-cleaned AG50W-X8 cation exchange resin (mesh 200-400) (Georg et al., 2006; as modified by de Souza et al., 2012). Si isotope ratios were measured on a *NuPlasma HR* MC-ICPMS (Nu Instruments) at GEOMAR equipped with an adjustable source-defining slit, which can be set to medium resolution to ensure separation of the ^{30}Si peak from molecular interferences. The measurements were carried out applying standard-sample bracketing (Albarède et al., 2004). All solutions were measured at a Si concentration of 14-21 µmol/kg of samples and standards depending on the performance of the instrument on the respective measurement day and were introduced into the plasma via a Cetac Aridus II desolvating nebulizer system equipped with a PFA nebulizer operated at a 60 to 80 µL/min uptake rate. Si isotope compositions are reported in the $\delta^{30}Si$ notation as deviations of the measured $^{30}Si/^{28}Si$ from the NIST standard NBS28 in parts per thousand (‰). Repeated measurements of the reference materials IRMM018 and Big Batch gave average $\delta^{30}Si$ values of -1.52 ± 0.18‰ ($2\sigma_{(sd)}$) and -10.84 ± 0.18‰ ($2\sigma_{(sd)}$), respectively, which are in good agreement with values obtained by other laboratories (Reynolds et al., 2007). Samples were measured three to five times within a one-day session and measurements were repeated on at least two separate days. The resulting uncertainties ranged between 0.04 and 0.23‰ ($2\sigma_{(sd)}$) (Tables 1, 2). Replicate measurements of an in-house diatom matrix standard over longer periods of time gave an external reproducibility of 0.11‰ ($2\sigma_{(sd)}$). Error bars provided in the figures correspond to that external reproducibility unless the uncertainties of the repeated sample measurements were higher.

2.2.2 Neodymium and Strontium Isotope Analyses

To obtain the radiogenic isotope composition of past bottom seawater at the sites of the sediment cores from the early diagenetic Fe-Mn coatings of the sediment particles, previously published methods were applied (Gutjahr et al., 2007; see supplement for details). The residual detrital material was leached repeatedly to remove remaining coatings and was then treated with a mixture of concentrated HF-HNO_3-HCl for total dissolution. The separation and purification of Nd and Sr in the leachates and in the completely dissolved detrital

sediment fraction followed previously published procedures for Nd (Cohen et al., 1988) and Sr (Horwitz et al., 1992) applying ion exchange chromatography for separation of Rb/Sr from the rare earth elements (REEs) (0.8 mL AG50W-X12 resin, mesh 200-400) followed by separation of Sr from Rb (50 µL Sr-Spec resin, mesh 50-100), and separation of Nd from the other REEs (2 mL Eichrom Ln-Spec resin, mesh 50-100). All radiogenic isotope measurements were performed on the *NuPlasma HR* MC-ICPMS (Nu Instruments) at GEOMAR. Measured Nd isotope compositions were corrected for instrumental mass bias using a $^{146}Nd/^{144}Nd$ of 0.7219 and were normalised to the accepted $^{143}Nd/^{144}Nd$ literature value of 0.512115 of the JNdi-1 standard (Tanaka et al., 2000). All values are given as ε_{Nd}, which corresponds to the measured $^{143}Nd/^{144}Nd$, normalised to the Chondritic Uniform Reservoir CHUR (0.512638), multiplied by 10,000. The external reproducibility was estimated by repeated measurements of the JNdi-1 standard and was always better than 20 ppm ($2\sigma_{(sd)}$, Tables 1, 2). Measured $^{87}Sr/^{86}Sr$ ratios were corrected for instrumental mass bias using $^{88}Sr/^{86}Sr = 8.3752$ and were normalised to the accepted value for NIST SRM987 of 0.710245. The $2\sigma_{(sd)}$ external reproducibility of repeated standard measurements was always better than 36 ppm ($2\sigma_{(sd)}$, Tables 1, 2). Procedural Nd and Sr blanks for leachates and total dissolutions of the detrital material were ≤ 83 pg and 2.1 ng, respectively, and thus negligible compared to the concentrations of the samples.

3 Results

3.1 Core M771-470 (Callao)

Sediment core M771-470 located at 11°S in 145 m water depth, is characterised by bSi concentrations between 10.1% and 26.9% and total N contents between 0.5% and 1.1% (Fig. 2a, Table 1), whereby the lowest values occurred just prior to the end of the LIA. The maximum bSi concentrations were found during the transition period. In contrast, the highest nitrogen (N) content occurred later in the youngest part of the record. The $\delta^{30}Si_{opal}$ varied between +0.6‰ and +1.1‰ (Fig. 2b) and followed bSi concentrations with the maximum and minimum isotope values corresponding to the same respective depths for both parameters.

The $\varepsilon_{Nd\ detritus}$ is characterised by values between -3.6 and -5.2 with a mean value of -4.5 ± 1.0 ($2\sigma_{(sd)}$) (Fig. 2c, Table 1). The $^{87}Sr/^{86}Sr_{detritus}$ signatures of the same samples range between 0.70647 and 0.70936 (Fig. 2d, Table 1). The variability of $\varepsilon_{Nd\ detritus}$ and $^{87}Sr/^{86}Sr_{detritus}$ is very

similar. Samples from the LIA show a trend towards more radiogenic $\varepsilon_{Nd\ detritus}$ and less radiogenic $^{87}Sr/^{86}Sr_{detritus}$. At the beginning of the transition period both records indicate a marked change to less radiogenic $\varepsilon_{Nd\ detritus}$ and more radiogenic $^{87}Sr/^{86}Sr_{detritus}$ values, which was more pronounced in the Sr than in the Nd isotope data, resulting in the youngest samples having the least radiogenic $\varepsilon_{Nd\ detritus}$ and the most radiogenic $^{87}Sr/^{86}Sr_{detritus}$ signatures.

In theory, the radiogenic isotope composition of authigenic Fe-Mn oxyhydroxide coatings is a useful tracer to detect changes on the prevailing bottom water masses at a distinct location. The PCUC, which dominates the bottom waters at the core locations today, is characterised by radiogenic ε_{Nd} signatures of -1.8 (Lacan and Jeandel, 2001; Grasse et al., 2012). A deepening of the nutricline and a vertical expansion of surface water masses during the LIA could change that value towards less radiogenic signatures typical for water masses originating from the South Pacific (Piepgras and Wasserburg, 1982; Grasse et al., 2012). However, as shown before (Ehlert et al., 2013) the authigenic coating fraction from sediments along the Peruvian shelf does not necessarily represent changes in water mass advection and is therefore not a reliable proxy (see also Supplement for details).

3.2 Core B0405-6 (Pisco)

In core B0405-6 located near 14°S off Pisco in 299 m water depth the range of bSi concentrations and its maximum value are higher than in core M771-470 and varied between 12.6% and 37.7% (Fig. 2e, Table 2). The trends are very similar to those of core M771-470 and bSi content correlates closely with the diatom accumulation rate (Fig. 2e). The lowest values of both parameters occurred at the end of the LIA and highest values were found right after the end of the LIA at the beginning of the transition period. The N content ranges from 0.5% around 1860 AD to 1.8% in the youngest sample of the record (Fig. 2e) (Gutiérrez et al., 2009) with maximum N content in core B0405-6 also being higher than in core M771-470. The $\delta^{30}Si_{opal}$ record shows the same range from +0.6‰ to +1.1‰ as core M77/1-470 and a very similar trend with the lowest values near the end of the LIA and the highest values immediately thereafter during the transition period (Fig. 2f, Table 3). The $\delta^{15}N_{sed}$ ranges between 3.6‰ and 7.6‰ and shows a trend from lower mean values around 4‰ to 5‰ during the LIA to higher values between 6‰ and 7‰ in the modern sediments (Fig. 2f).

The $\varepsilon_{Nd\ detritus}$ signatures are characterised by overall somewhat more radiogenic values than of core M771-470 ranging from -4.1 to -2.5 (mean value -3.2 ± 0.9, $2\sigma_{(sd)}$ excluding the value of -0.2 ε_{Nd} at 1761 AD, which is considered an outlier), with slightly less radiogenic values in the older part of the record and more radiogenic values in the younger part (Fig. 2g, Table 2). The $^{87}Sr/^{86}Sr_{detritus}$ values range between 0.70711 and 0.70796 (Fig. 2h, Table 2). Similar to core M771-470 although less pronounced, the main feature in the detrital Sr isotope record observed is a trend from less radiogenic $^{87}Sr/^{86}Sr_{detritus}$ values in the older part of the record towards more radiogenic values in the youngest part with a shift at the end of the LIA and during the early transition period.

4 Discussion

After the end of the LIA around 1820 AD the mean position of the ITCZ shifted northward (Sachs et al., 2009) causing an intensification of alongshore winds and enhanced coastal upwelling off the Peruvian coast (Sifeddine et al., 2008; Gutiérrez et al., 2009), diminished coastal sea surface temperatures (Vargas et al., 2007), and a decrease in precipitation on land (Rabatel et al., 2008; Bird et al., 2011). Records of productivity and redox conditions based on $\delta^{15}N_{sed}$ and the Mo and Cd content of the sediments indicate a rapid change of the biogeochemical composition of the source waters to higher nutrient concentrations causing higher biological productivity and lower subsurface oxygen, which have persisted until the present day (Sifeddine et al., 2008; Gutiérrez et al., 2009; Salvatteci et al., 2014a). The shift after the end of the LIA constitutes a major anomaly of late Holocene climate in the Eastern Pacific, which was of the same order of magnitude as the changes in conditions off Chile during the Younger Dryas (De Pol-Holz et al., 2006). This study focuses on the reconstruction of the regime shift from the LIA and a transitional period towards modern conditions and its controlling factors including the evolution of nutrient utilisation and changes in the advection of water masses and material transport.

4.1 Changes in Biological Productivity and Nutrient Consumption

4.1.1 Evolution of Surface Water Productivity and Nutrient Utilisation

The pronounced change in the biogeochemical regime from low productivity during the LIA to higher productivity during the transitional and modern period thereafter is documented by several sedimentary records from the EEP region and has been dated at ~1820 AD (Sifeddine et al., 2008; Gutierrez et al., 2009; Díaz-Ochoa et al., 2009, 2011; Salvatteci et al., 2014a). Similarly, both cores M771-470 from 11°S and B0405-6 from 14°S off Pisco show the characteristic coeval pronounced increase in bSi and total N content (Figs. 2a, e) and C_{org} concentration (not shown here) after the end of the LIA and during the transition period. Therefore, three time periods that show distinct differences in productivity and nutrient utilisation have been identified from our records and will be discussed in the following: the LIA, the transition period from the LIA to modern conditions between ~1820 and ~1870AD, and modern conditions after ~1870 AD.

Both cores recorded a two- to threefold increase in bSi content from 10-12% prior to the end of the LIA to values of up to 27% in M771-470 and up to 38% in B0405-6 during the transition period (Figs. 2a, e). Afterwards the bSi contents decreased again but have remained at a level of ~20% and thus significantly higher than prior to the end of the LIA. The increase in bSi content is also reflected by a marked increase in diatom accumulation rate in core B0405-6 (Fig. 2e) (Gutiérrez et al., 2009). Analyses of the downcore diatom assemblages have shown that the high diatom accumulation rates and bSi content in core B0405-6 during the transition period were associated with diatom layers dominated by *Skeletonema costatum* (Gutiérrez et al., 2009), a species that is today more abundant when upwelling is more intense during Austral winter/spring.

Both cores are characterised by a very high correlation between total N and C_{org} content (r^2=0.95 for core M771-470 and 0.8 for core B0405-6, respectively) (Gutiérrez et al., 2009; this study). In contrast, bSi and total N contents do not co-vary throughout the records (Fig. 3a). Surface sediments from the Peruvian shelf region between the Equator and ~18°S show a relatively weak but positive correlation between bSi and N contents (r^2 = 0.5, Fig. 3a) (Ehlert et al., 2012; Mollier-Vogel et al., 2012). Similar to the surface sediments, bSi and total N concentrations in core M771-470 are positively correlated, whereas they essentially do not correlate in core B0405-6. This is because the bSi maximum at the end of the transition period was more pronounced in core B0405-6 and higher than surface sediment bSi contents anywhere along the shelf region off Peru. At the same time only a rather gradual increase in total N content with some excursions to low values during the transition period occured (Figs.

2a, e). The total N concentration also did not always co-vary with $\delta^{15}N_{sed}$ (Fig. 3c). In particular, the samples from the late transition period show very low total N concentrations but high $\delta^{15}N_{sed}$, high $\delta^{30}Si_{opal}$ and bSi content.

Sedimentary $\delta^{15}N_{sed}$ data, which are only available for core B0405-6, show a shift from lower values around +4‰ to +5‰ during the LIA to higher values around +7‰ after the end of the LIA and have remained at that level since then (Fig. 2f) (Gutiérrez et al., 2009). The values in the younger part of the record are in good agreement with surface sediment $\delta^{15}N_{sed}$ data measured in the main Peruvian upwelling region ranging from +6‰ to +9‰ (Mollier-Vogel et al., 2012). Bulk $\delta^{15}N_{sed}$ signatures measured in core B0405-13 from 12°S (184 m water depth) close to the location of core M771-470 can be used for comparison and show very similar values, amplitude, and variability as core B0405-6 (Fig. 2i) (Gutiérrez et al., 2009). In contrast to $\delta^{15}N_{sed}$, the $\delta^{30}Si_{opal}$ signatures, which mainly reflect changes in surface water nutrient utilisation, are not only characterised by a simple increase at the end of the LIA. Instead, both $\delta^{30}Si_{opal}$ records closely follow the evolution of the bSi concentrations and show intermediate $\delta^{30}Si_{opal}$ signatures between +0.8‰ and +0.9‰ during the LIA, a pronounced short-term decrease to +0.6‰ at the end of the LIA, which was followed by a marked increase to values around +1.1‰ during the transition period, and finally a return to intermediate values between +0.8‰ and +1.0‰ in the modern part of the records (Figs. 2b, f). The correspondence between bSi content and $\delta^{30}Si_{opal}$ is more pronounced in core B0405-6 (Fig. 3b), which shows a higher variability and amplitude of bSi content. The difference in the $\delta^{30}Si_{opal}$, $\delta^{15}N_{sed}$, bSi and total N content records during the transition from LIA to modern conditions reflects the different environmental factors controlling the proxies, which will be discussed in the following sections.

4.1.2 Present Day Surface Water Utilisation versus Subsurface Nitrate Loss

Diatoms are the dominant phytoplankton group of the Peruvian upwelling region (Estrada and Blasco, 1985; Bruland et al., 2005). The $\delta^{30}Si_{opal}$ of these diatoms is primarily controlled by surface water diatom productivity and $Si(OH)_4$ utilisation (De La Rocha et al., 1998; Brzezinski et al., 2002; Egan et al., 2012). Off Peru the $\delta^{30}Si_{opal}$ has also been shown to be dependent on the isotopic signature of the advected surface and subsurface water masses (Ehlert et al., 2012; Grasse et al., 2013). Similarly, the $\delta^{15}N_{sed}$ of the organic matter is

mm mpi 11/17/14 10:06 AM
Deleted: but o

controlled by N isotope fractionation during NO_3^- uptake by phytoplankton, mostly diatoms. Off Peru, however, the NO_3^- supplied to the surface waters has previously been enriched in $^{15}NO_3^-$ due to upwelling of oxygen-depleted subsurface waters, which had undergone significant NO_3^--loss processes (mostly denitrification, but also anammox processes, associated with a high fractionation of up to 20-30‰) (Lam et al., 2009; Altabet et al., 2012). Bulk sediment $\delta^{15}N_{sed}$ in areas with oxygen-depleted waters is therefore usually interpreted to reflect changes in the intensity of subsurface NO_3^- reduction and the extent and strength of the oxygen minimum zone (Altabet et al., 1999; De Pol-Holz et al., 2007; Agnihotri et al., 2008; Gutiérrez et al., 2009). The direct comparison of $\delta^{30}Si_{opal}$, reflecting mostly utilisation, and $\delta^{15}N_{sed}$, reflecting both utilisation and NO_3^- reduction, from core B0405-6 off Pisco will therefore provide insights into the strength of NO_3^- reduction in the past.

Subsurface water column $\delta^{15}N_{NO3-}$ data from the present-day Peruvian shelf are isotopically very heavy, in particular along the southern shelf region between 10°S and 17°S, where values of up to +25‰ are reached due to the increasing oxygen deficit and intensification of NO_3^--loss processes (Mollier-Vogel et al., 2012; Altabet et al., 2012). These isotopically enriched waters are upwelled along the shelf and represent the source for organic matter production in the surface waters. Therefore, it is expected, that the deposited sedimentary organic matter reflects these enriched subsurface water signatures. However, the latitudinal increase in surface sediment $\delta^{15}N_{sed}$ from the same shelf region to maximum mean values around +9‰ is much lower than that measured in the water column (Mollier-Vogel et al., 2012). The reason for this observation is that the $\delta^{15}N_{sed}$ signal in the southern shelf region (10-17°S) did not fully record the the $^{15}NO_3^-$ enrichment in the water column but is a combination of the isotopic effects associated with subsurface NO_3^--loss and incomplete surface water NO_3^- utilisation and water mass mixing. Direct comparison of $\delta^{30}Si_{opal}$ and $\delta^{15}N_{sed}$ allows to investigate and to distinguish the relative importance of these processes (Fig. 4a). Diatoms off Peru preferentially take up $Si(OH)_4$ and NO_3^- at a ratio of ~1:1 or below (Brzezinski, 1985; Takeda, 1998; Hutchins et al., 2002). If utilisation were the only driving factor, the sedimentary $\delta^{30}Si_{opal}$ and $\delta^{15}N_{sed}$ should all plot close to a line that reflects the enrichment during increasing utilisation, i.e. 1.1‰ for $\delta^{30}Si_{opal}$ (De La Rocha et al., 1997) and ~5‰ for $\delta^{15}N$ (DeNiro and Epstein, 1981; Minagawa and Wada, 1984). Under the influence of denitrification with an enrichment of ~20‰ (Lam et al., 2009), however, the relationship between $\delta^{30}Si_{opal}$ and $\delta^{15}N_{sed}$ would be very different (Fig. 4a).

Most modern shelf samples plot either on or above the theoretical curve for utilisation implying, if at all, $Si(OH)_4$ limiting conditions (Fig. 4a). Very few samples are shifted towards the theoretical curve for denitrification, indicating a weak influence of NO_3^--loss processes on the preserved isotope signatures. Especially along the central shelf region (green curves in Fig. 4a), where the cores are located, surface sediment signatures closely reflect the utilisation in surface waters with only little influence of NO_3^--loss in the water column and sediments.

4.1.3 Past Surface Water Utilisation versus Subsurface Nitrate Loss

Assuming that source water isotope composition (+1.5‰ $\delta^{30}Si_{Si(OH)4}$, +9‰ $\delta^{15}N_{NO3}$) and isotope enrichment during utilisation and denitrification (-1.1‰ $\delta^{30}Si_{opal}$, ~-5‰ and ~-20‰ $\delta^{15}N_{NO3-}$ for utilisation and denitrification, respectively) in the past were similar to the conditions of the present-day shelf region (Ehlert et al., 2012; Mollier-Vogel et al. 2012), the samples of core B0405-6 indicate variable utilisation/NO_3^--loss conditions (Fig. 4b). Samples from the LIA and the transition period generally plot on or above the utilisation curve indicating stronger $Si(OH)_4$ than NO_3^- utilisation. This implies that in the Peruvian upwelling system has rather been a $Si(OH)_4$-limited system during that time, similar to today (Fig. 4a). During the transition period, when strong upwelling conditions caused intense blooming of *Skeletonema costatum*, utilisation of $Si(OH)_4$ and NO_3^- was very close to a 1:1 ratio. In contrast, the samples from the end of the LIA and especially the recent samples are shifted slightly towards the denitrification curve indicating a higher influence of NO_3^--loss processes. This is particularly the case for the samples from the end of the LIA, which have the lowest $\delta^{30}Si_{opal}$ but at the same time already show a strong increase in $\delta^{15}N_{sed}$ to values of near +6‰. The most likely explanation is that upwelling was strongly increased during those brief periods resulting in high nutrient supply, high productivity, and either more complete NO_3^- utilisation (Gutiérrez et al., 2009) or increased NO_3^--loss caused by enhanced subsurface oxygen depletion. Overall, however, the utilisation signal appears to have dominated both the Si and N isotope records.

If, however, the $\delta^{15}N_{sed}$ is dominated by utilisation it is interesting that in the cores (both B0405-6 and -13) $\delta^{15}N_{sed}$ and proxies for sediment redox conditions (e.g. molybdenum concentrations) are strongly coupled throughout the record (Sifeddine et al., 2008; Gutiérrez

mm mpi 11/3/14 9:32 AM
Deleted: also

et al., 2009). One direct interpretation could be that the diatom blooms, and subsequently the degradation of the organic matter, strongly control the oxygen availability in the sediments after sedimentation and burial. Therefore, increased diatom productivity and higher $Si(OH)_4$ and NO_3^- utilisation would result in an increase in $\delta^{15}N_{sed}$. At the same time more oxygen is consumed during degradation of the organic matter in the sediments causing more reducing conditions in the sediments. Consequently, a change in the subsurface water column structure, e.g. enhanced re-supply of oxygen via ocean currents, may not be reflected in the $\delta^{15}N_{sed}$ record.

4.1.4 Modelling the Surface Water Utilisation

Following the above considerations we will try to quantify past utilisation based on our data. The theoretical relationship between the degree of surface water nutrient utilisation and the stable isotope composition of Si and N can be described assuming either Rayleigh-type (single input followed by no additional nutrients newly supplied to a particular parcel of water followed by fractional loss as a function of production and export) or steady state (continuous supply and partial consumption of nutrients causing a dynamic equilibrium of the dissolved nutrient concentration and the product) fractionation behaviour (Fig. 5) (Mariotti et al., 1981). The lighter isotopes are preferentially incorporated into the diatom frustules and the organic matter, respectively, leaving the dissolved fraction enriched in the heavier isotopes (Wada and Hattori, 1978; Altabet et al., 1991; De La Rocha et al., 1997). The fractionation between $\delta^{30}Si$ in seawater and $\delta^{30}Si$ in the produced diatom opal has generally been assumed to be -1.1‰ (De La Rocha et al., 1997) whereas between $\delta^{15}N_{NO3-}$ of seawater and $\delta^{15}N$ of the newly formed organic matter it is usually between -3‰ to -6‰ (DeNiro and Epstein, 1981; Minagawa and Wada, 1984). Here we adopted -5‰, which corresponds to present-day conditions along the central Peruvian shelf (Mollier-Vogel et al., 2012).

Along the Peruvian shelf region biological productivity in the euphotic zone is mainly driven by upwelling of nutrients from subsurface waters. For the calculation of the utilisation of these nutrients, an initial $\delta^{30}Si_{Si(OH)4}$ of +1.5‰ (Ehlert et al., 2012) and an initial $\delta^{15}N_{NO3-}$ of +9‰ (Mollier-Vogel et al., 2012) for the upwelled water masses at 14°S is assumed. The lower mean $\delta^{15}N_{sed}$ of about +5‰ and $\delta^{30}Si_{opal}$ of +0.7‰ signatures during the LIA in the southerly core B0405-6 correspond to a dissolved $\delta^{15}N_{NO3-}$ and $\delta^{30}Si_{Si(OH)4}$ isotope signature

435 of the surface waters of +10‰ and +1.8‰ and a calculated NO_{3^-} and $Si(OH)_4$ utilisation of
436 only 20-30% for steady state-type fractionation (Fig. 5b) and 35-50% for Rayleigh-type
437 fractionation (Fig. 5a) behaviour, respectively. The highest mean values of +1.1‰ for $\delta^{30}Si_{opal}$
438 and +6.8‰ for $\delta^{15}N_{sed}$ for the transition period correspond to a much higher utilisation of
439 ~60% for steady state-type fractionation and ~80% assuming Rayleigh-type fractionation.
440 Consequently, the calculated utilisation of available $Si(OH)_4$ and NO_3^- more than doubled,
441 whereby bSi concentrations and diatom accumulation rates increased by about a factor of
442 three (Fig. 2e).

443 The changes in $Si(OH)_4$ and NO_3^- utilisation were of the same order of magnitude and reflect
444 low nutrient utilisation during the LIA and much higher degree of utilisation thereafter. The
445 large increase in $\delta^{15}N_{sed}$ at the end of the LIA has been interpreted to reflect an expansion of
446 nutrient-rich, oxygen-poor subsurface waters (Gutiérrez et al., 2009). However, comparison
447 with $\delta^{30}Si_{opal}$ shows that indeed the increase in $\delta^{15}N_{sed}$ may have occurred as a consequence of
448 the extension of the oxygen minimum zone and increasing subsurface NO_3^--loss but can also
449 be explained by higher surface water utilisation. As Mollier-Vogel et al. (2012) have shown,
450 the subsurface enrichment of $\delta^{15}N_{NO3-}$ caused by NO_3^--loss processes can only be reflected in
451 the sediments under near-complete surface water NO_3^- utilisation, which did obviously not
452 occur at our studied sites.

453 In the modern samples the $\delta^{30}Si_{opal}$ are characterised by a slight decrease after the transition
454 period from mean value of +1.12‰ to +0.82‰, whereas the $\delta^{15}N_{sed}$ values remain at the same
455 level around +7‰ (Fig. 2). This corresponds to a ~20% higher NO_3^- than $Si(OH)_4$ utilisation
456 (Fig. 5). However, when assuming that diatoms are the dominating primary producers with a
457 NO_3^-:$Si(OH)_4$ uptake ration of ~1, these 20% could be interpreted to reflect the increase in
458 subsurface NO_3^--loss that is not observable during the LIA or the transition period. I.e. during
459 the LIA and the transition period utilisation was the domniating process influencing the
460 $\delta^{15}N_{sed}$ signal, whereas during modern times NO_3^--loss enhanced the signal. By combining the
461 $\delta^{30}Si_{opal}$ and the $\delta^{15}N_{sed}$ records this "additional" signal can be quantified here: if only
462 utilisation would play a role the expected $\delta^{15}N_{sed}$ signal would be ~+6‰ (corresponding to the
463 measured ~+0.8‰ for $\delta^{30}Si_{opal}$, Fig. 5). The additional 1‰ $\delta^{15}N_{sed}$ must be due to NO_3^--loss.

464 The overall relatively low $\delta^{30}Si_{opal}$ signatures between 0.8‰ and 1.0‰ during the LIA and in
465 the modern part of the records (Figs. 2, 5) document that the utilisation of $Si(OH)_4$ only

changed slightly during the investigated period of time although the accumulation rate of produced diatoms was much higher after the LIA (Fig. 2e) (Gutiérrez et al., 2009). This suggests that the nutrient concentrations in the upwelled subsurface source waters must have been lower during the LIA than they are today. During the LIA large-scale circulation changes, i.e. a weak Walker circulation and a contraction of the SPSH (Conroy et al., 2008; Lamy et al., 2001), caused permanent El Niño-like conditions along the Peruvian upwelling system. During such conditions, the alongshore winds weakened and caused a deepening of the thermo-, oxy- and nutricline, and therefore a reduction of vertical pumping of nutrient-rich and oxygen-depleted subsurface waters off Peru. Such a reduced nutrient supply to the euphotic zone from subsurface waters resulted in an increase in nutrient deficit in surface waters and decreased biological productivity. Enhanced water column oxygenation and lower organic matter flux led to decreased organic matter preservation in the sediments.

4.1.5 Factors Influencing the Reconstruction of the Utilisation Signals

mm mpi 11/17/14 10:16 AM
Comment [1]: The following section has been restructured (without changing the content) in order to highlight the connection to the following section 4.2.

There are two main factors that can influence the reconstruction of nutrient utilisation in the past: 1) a change in the dominating diatom assemblages has to be considered and 2) the interpretation strongly depends on the assumptions for the environmental conditions, e.g. source water signature and isotope enrichment during utilisation.

Varying upwelling and nutrient supply conditions also cause changes in the dominating diatom assemblages. Recent results from culturing experiments suggest species-dependent enrichment factors for diatom-δ^{30}Si (-0.5‰ to -2.1‰; Sutton et al., 2013) and also diatom frustule-bound δ^{15}N (-1.9‰ to -11.2‰; Horn et al., 2011). This raises the question whether a change in diatom assemblages may have been the cause for the observed downcore $\delta^{30}Si_{opal}$ and, to a lesser extent, the bulk $\delta^{15}N_{sed}$ variations. The quasi-monospecific diatom layers from the transition period 1820-1870 AD consist mainly of *Skeletonema costatum* (Gutiérrez et al., 2009), for which an enrichment factor ε of -1.0‰ similar to the applied -1.1‰ was determined (De la Rocha et al., 1997). The younger sediments also also contain abundant upwelling-indicative species such as *Thalassionema nitzschioides* and *Chaetoceros sp.* (Abrantes et al., 2007), whereby *Chaetoceros brevis*, a species from the Southern Ocean, has been shown to have a much higher ε of -2.1‰ (Sutton et al., 2013). That means, assuming the same surface water $\delta^{30}Si_{Si(OH)4}$ signatures, a dominance of *Chaetoceros sp.* in the sediments

should result in a lower $\delta^{30}Si_{opal}$ whereas assemblages dominated by *Skeletonema costatum* should be characterised by higher $\delta^{30}Si_{opal}$ signatures, which is exactly what core B0405-6 shows. Consequently, the difference in $\delta^{30}Si_{opal}$ over time could reflect the change in diatom assemblage and not a change in nutrient utilisation. On the other hand, *Chaetoceros brevis* is a polar species and it is not clear whether off Peru it undergoes the same high fractionation factor during frustule growth. It has been shown that the offset between modern surface water $\delta^{30}Si_{Si(OH)4}$ and surface sediment $\delta^{30}Si_{opal}$ along the central Peruvian shelf is between -1.1‰ and -1.3‰ (Ehlert et al., 2012), which indicates that either the enrichment factor for the dominating *Chaetoceros* species off Peru does not deviate significantly from -1.1‰ or that the mixing of different diatoms in the sediment samples overprints any isotopic excursions of single species caused by higher or lower fractionation factors. Given the paucity of data on the fractionation factors for the dominant diatom species off Peru, the importance of the role of downcore changes in the assemblage composition is hard to determine.

The assumed source water $\delta^{30}Si_{Si(OH)4}$ and $\delta^{15}N_{NO3-}$ values of +1.5‰ and +9‰ (Figs. 5, 6), respectively, were measured in the present day subsurface waters under strong upwelling conditions during which high amounts of nutrients are supplied to the euphotic zone (Ehlert et al., 2012; Mollier-Vogel et al., 2012). Under strong upwelling conditions the bottom waters on the shallow shelf are today dominated by the southward directed high-nutrient Peru-Chile Undercurrent (PCUC) (Fig. 1) (Brink et al., 1983). Under LIA-conditions (prevailing El Niño-like conditions), however, atmospheric and oceanic circulation was different; the nutricline was deeper as a consequence of a weak Walker circulation and the winds driving the upwelling were weaker as a consequence of the SPSH contraction (Salvatteci et al. 2014a). In fact, the pumped waters were likely nutrient-depleted, because the Ekman layer did not reach the subsurface nutrient-rich waters. Under these conditions, the subtropical and equatorial nutrient-depleted surface water masses may have occupied the entire surface layer in the coastal realm because they expanded both latitudinally and vertically in the water column (Montes et al., 2011). This may have changed the source water isotopic signatures and would therefore also change the calculated degrees of utilisation. If, for example, the assumed source water $\delta^{15}N_{NO3-}$ was +6‰ instead of +9‰ (e.g. due to weaker subsurface NO_3^--loss and weaker ^{15}N enrichment during the LIA) the downcore $\delta^{15}N_{sed}$ data of core B0405-6 would all plot closer to the denitrification curve (Fig. 4b). Redox proxies from the records, indeed, indicate a weaker OMZ (Gutiérrez et al., 2009), which would make a lower $\delta^{15}N_{NO3-}$

in source waters likely. However, to date there is no reliable information if and how much the source water $\delta^{30}Si_{Si(OH)4}$ and $\delta^{15}N_{NO3-}$ signatures changed over time.

In the following we thus investigate variations in past water mass circulation, upwelling conditions, as well as material input and transport to reconstruct the source water conditions without considering the potential influence of changes in diatom assemblages.

4.2 Changes in Water Mass Circulation, Detrital Material Input and Transport

The radiogenic isotope composition of the lithogenic particles ($\varepsilon_{Nd\ detritus}$ and $^{87}Sr/^{86}Sr_{detritus}$) of the sediments provides useful information about the source region of material and therefore about changes in material input and transport, either eolian or via ocean currents (e.g. Grousset et al., 1988). Surface sediments along the Peruvian shelf show highly variable signatures, which have overall more radiogenic $\varepsilon_{Nd\ detritus}$ values in the North and much less radiogenic $\varepsilon_{Nd\ detritus}$ values in the South off southern Peru and northern Chile (Ehlert et al., 2013). This north-south trend is a consequence of the southward increasing contributions of material input from the adjacent Andean hinterland rocks. The Andean rocks along the northwestern South American region display a wide range in ε_{Nd} and $^{87}Sr/^{86}Sr$ signatures (Fig. 6) (Sarbas and Nohl, 2009) varying from highly radiogenic ε_{Nd} around 0 and unradiogenic $^{87}Sr/^{86}Sr$ values around 0.704 in the equatorial region in northern Peru to much less radiogenic ε_{Nd} mostly below -4 and more radiogenic $^{87}Sr/^{86}Sr$ mostly above 0.705 in southern Peru and northern Chile. The sedimentary $\varepsilon_{Nd\ detritus}$ and $^{87}Sr/^{86}Sr_{detritus}$ records of the two cores off Callao at 11°S and off Pisco at 14°S show broad similarities, but also some differences. Both cores recorded a significant change in $\varepsilon_{Nd\ detritus}$ and $^{87}Sr/^{86}Sr_{detritus}$, and therefore a change in provenance, at the end of the LIA and during the transition period. Core M771-470, although being located further north, is overall characterised by less radiogenic $\varepsilon_{Nd\ detritus}$ values than core B0405-6 (Figs. 2, 6). The $\varepsilon_{Nd\ detritus}$ of core M771-470 recorded a trend from less radiogenic towards more radiogenic values prior to the end of the LIA, followed by a step of 1.5 ε_{Nd} units towards less radiogenic values, which afterwards remained at that level. In contrast, the $\varepsilon_{Nd\ detritus}$ record of core B0405-6 remained at a level around -3.6 during the LIA and then slightly increased to maximum values of up to -2.5 in the younger part. The $^{87}Sr/^{86}Sr_{detritus}$ record in both cores is mainly characterised by a rapid shift towards more radiogenic values at the end of the LIA, whereby the change was much more pronounced in

core M771-470 (Figs. 2d, h). The youngest samples of the cores are in good agreement with measurements of surface sediments from the same area (Figs. 2, 6) (Ehlert et al., 2013). The variability in core M771-470 display the same magnitude as the complete glacial-interglacial variation in core SO147-106KL located at 12°S off Lima (Ehlert et al., 2013). All data of both M771-470 and B0405-6 plot within the provenance fields of southern Peru and northern Chile (Fig. 6).

Today, material input along the Peruvian shelf occurs mostly via riverine and minor eolian input (Molina-Cruz, 1977; Scheidegger and Krissek, 1982). The LIA, however, was characterised by wetter conditions (Haug et al., 2001; Gutiérrez et al., 2009). These changes in precipitation were associated with the position of the ITCZ, changes in Walker ciculation, and expansion/contraction of the South Pacific Subtropical High (SPSH) (Salvatteci et al., 2014a). Additionally, there has been a tight connection to northern hemisphere climate. Speleothem records from the central Peruvian Andes for example indicate a pronounced link to North Atlantic climate (Kanner et al., 2013). During cold periods like the LIA, the Peruvian upwelling region exhibited an El Niño-like mean state (Salvatteci et al., 2014a) due to the mean southward migration of the ITCZ and the associated precipitation belt, which also caused more intense rainfall in the central Andean hinterland (Rabatel et al., 2008; Reuter et al., 2009). Most terrigenous particles and weathering products such as clay minerals from the LIA show indications of increased riverine transport and discharge (Sifeddine et al., 2008; Salvatteci et al., 2014a). Consequently, material input during the LIA was dominated by local sources due to the higher river discharge.

After the end of the LIA the region experienced a northward displacement of the ITCZ and the northern rim of the SPSH to their modern position, coupled with an enhancement of the atmospheric Walker circulation (Gutiérrez et al., 2009). The climate in the EEP became drier and alongshore winds became stronger, riverine input diminished and eolian dust input increased. The wind-blown dust has mainly originated from the Atacama Desert located in the southern Peruvian and northern Chilean Andes (Molina-Cruz, 1977). This material has less radiogenic ε_{Nd} and much more radiogenic $^{87}Sr/^{86}Sr$ values (Fig. 6) (Sarbas and Nohl, 2009). The record of core M771-470 is in agreement with this. The LIA-sediments indicate a local origin, probably via riverine input, whereas the younger sediments display characteristics from a more southerly origin and therefore increased eolian sources, possibly from the Atacama Desert. The signatures and overall small variations in core B0405-6 are much more

mm mpi 11/3/14 2:32 PM
Deleted: ,

mm mpi 11/3/14 2:32 PM
Deleted: when t

difficult to interpret. There are fewer rivers in Southern Peru around Pisco compared to the Callao region. Therefore, riverine-derived material from northern and central Peru, which is transported via the PCUC, can get dispersed further south and can be deposited in the Pisco region. On the other hand, the influence of eolian deposition should be much higher at the southern core location. During the LIA river input increased in southern Peru as well, whereas eolian deposition was low. The invariate signature observed might be the result of mixing of sediment from the different sources. Also, in comparison to core M771-470 core B0405-6 is located much closer to the coast, which most likely diminished the differences in material input and transport between the LIA- and modern conditions.

In summary, our combined proxy information coherently hints to the same controlling processes that we already identified on glacial-interglacial timescales (Ehlert et al., 2013) and to different ENSO pattern during the LIA (enhanced El Niño-like conditions) and in modern times (La-Nina-like conditions). The locally sourced radiogenic isotope signatures show that during the LIA precipitation and runoff from the hinterland was higher but this could not compensate for the lower nutrient supply via diminished upwelling. Eolian wind forcing was low and the source waters of the upwelling carried less nutrients. Consequently, diatom productivity and nutrient utilisation were low. In contrast, after the end of the LIA radiogenic isotopes indicate diminished river runoff and increased dust transport, which is in agreement with an overall drier climate, probably driven by an expansion of the SPSH, and a shoaling of the thermocline/nutricline due to a stronger atmospheric Walker circulation. Especially in more recent times, the efficient remineralisation of nutrients from subsurface waters fuelled enhanced diatom productivity most liekly responsible for higher nutrient utilisation in surface waters as well as enhanced oxygen demand and NO_3^--loss in subsurface waters.

5 Conclusions

Proxies of productivity, nutrient utilisation and material provenance (bSi and N content, $\delta^{30}Si_{opal}$, $\delta^{15}N_{sed}$, $\varepsilon_{Nd\ detritus}$, and $^{87}Sr/^{86}Sr_{detritus}$) from two cores from the Peruvian shelf recorded significant changes in surface water $Si(OH)_4$ and NO_3^- concentration and utilisation due to changes in upwelling intensity and nutrient supply. During the LIA the overall nutrient content in the water column and in surface waters was low because the upwelling source waters contained less nutrients. Consequently, the Peruvian upwelling regime was

characterised by persistently reduced primary productivity. The reasons for this were most likely a contraction of the South Pacific Subtropical High and a weaker Walker circulation that resulted in a weakening of alongshore winds and a deepening of the nutricline.

The enhanced rainfall associated with higher moisture on land during prevailing El Niño-like conditions during the LIA were recorded by the radiogenic isotope composition of the detrital material along the shelf, which was mainly transported via rivers from the Andean hinterland. At the end of the LIA, in accordance with a northward shift of the ITCZ and an intensification of wind strength a higher dust transport of particles associated with drier conditions and eolian forcing is reflected by the radiogenic isotope composition of the detrital sediments. These conditions were also reflected in increasing upwelling strength, a rapid shoaling of the thermocline and nutricline, as well as enhanced nutrient supply and productivity to the surface waters. During a transition period a marked increase in diatom blooming events doubled the $Si(OH)_4$ and NO_3^- utilisation compared to the LIA, and was also higher than present day utilisation. After that transition period more persistent non-El Niño conditions favoured a high productivity accompanied by moderate utilisation of nutrients. Utilisation was similar to the LIA but productivity was much higher, which reflects the much higher concentrations of nutrients in surface waters.

Most studies of past coastal upwelling regions have argued so far that the sedimentary $\delta^{15}N_{sed}$ records were dominated by the large N isotope fractionation signature occurring during NO_3^--loss processes (denitrification or anammox) in oxygen-depleted subsurface waters upwelling. Comparison between $\delta^{30}Si_{opal}$ and $\delta^{15}N_{sed}$ in the same sediment samples of our study and assuming similar source water signatures as today, however, indicate that except for the period of time since ~1870 AD, the $\delta^{15}N_{sed}$ signatures to a large extent reflect expected utilisation signals, which has important implications for the reconstruction of variations in the intensity of oxygen depletion, the N cycle of the past and its controlling factors.

Acknowledgements

This work is a contribution of Sonderforschungsbereich 754 "Climate - Biogeochemistry Interactions in the Tropical Ocean" (www.sfb754.de), which is supported by the Deutsche Forschungsgemeinschaft. We acknowledge the help of Jutta Heinze in the laboratory of GEOMAR for the biogenic opal concentration measurements. We thank Ulrike

656 Lomnitz and Klaus Wallmann for their help with the ^{210}Pb dating and the establishment of the
657 age model of core M771-470.

658

659 **References**

660 Abrantes, F., Lopes, C., Mix, A. C., and Pisias, N. G.: Diatoms in Southeast Pacific surface
661 sediments reflect environmental properties, Quaternary Science Reviews, 26, 155–169, 2007.
662 doi:10.1016/j.quascirev.2006.02.022

663 Agnihotri, R., Altabet, M. A., Herbert, T. D., and Tierney, J. E.: Subdecadally resolved
664 paleoceanography of the Peru margin during the last two millennia, Geochemistry
665 Geophysics Geosystems, 9(Q05013), 2008. doi:10.1029/2007GC001744

666 Albarède, F., Telouk, P., Blichert-Toft, J., Boyet, M., Agranier, A., and Nelson, B.: Precise
667 and accurate isotopic measurements using multiple-collector ICPMS, Geochimica et
668 Cosmochimica Acta, 68(12), 2725–2744, 2004. doi:10.1016/j.gca.2003.11.024

669 Altabet, M. A., Deuser, W. G., Honjo, S., and Stienen, C.: Seasonal and depth-related changes
670 in the source of sinking particles in the North Atlantic, Nature, 354, 136–139, 1991.

671 Altabet, M. A., and Francois, R.: Sedimentary nitrogen isotopic ratio as a recorder for surface
672 ocean nitrate utilisation, Global Biogeochemical Cycles, 8(1), 103–116, 1994.

673 Altabet, M. A., Pilskaln, C., Thunell, R. C., Pride, C. J., Sigman, D. M., Chavez, F. P., and
674 Francois, R.: The nitrogen isotope biogeochemistry of sinking particles from the margin of
675 the Eastern North Pacific, Deep-Sea Research I, 46, 655–679, 1999.

676 Altabet, M. A., Ryabenko, E., Stramma, L., Wallace, D. W. R., Frank, M., Grasse, P., and
677 Lavik, G.: An eddy-stimulated hotspot for fixed nitrogen-loss from the Peru oxygen minimum
678 zone, Biogeosciences, 9(12), 4897–4908, 2012. doi:10.5194/bg-9-4897-2012

679 Bird, B. W., Abbott, M. B., Vuille, M., Rodbell, D. T., Stansell, N. D., and Rosenmeier, M.
680 F.: A 2,300-year-long annually resolved record of the South American summer monsoon
681 from the Peruvian Andes, PNAS, 108(21), 8583–8588, 2011. doi:10.1073/pnas.1003719108

682 Brink, K. H., Halpern, D., Huyer, A., and Smith, R. L.: The Physical Environment of the
683 Peruvian Upwelling System, Progress in Oceanography, 12, 285–305, 1983.

684 Bruland, K. W., Rue, E. L., Smith, G. J., and DiTullio, G. R.: Iron, macronutrients and diatom
685 blooms in the Peru upwelling regime: brown and blue waters of Peru, Marine Chemistry, 93,
686 81–103, 2005. doi:10.1016/j.marchem.2004.06.011

687 Brzezinski, M. A.: The Si:C:N ratio of marine diatoms: interspecific variability and the effect
688 of some environmental variables, Journal of Phycology, 21(3), 347–357, 1985.

689 Brzezinski, M. A., Pride, C. J., Franck, V. M., Sigman, D. M., Sarmiento, J. L., Matsumoto,
690 K., Gruber, N., Rau, G. H., and Coale, K. H.: A switch from Si(OH)4 to NO3- depletion in
691 the glacial Southern Ocean, Geophysical Research Letters, 29(12), 3–6, 2002.
692 doi:10.1029/2001GL014349

693 Codispoti, L. A., Brandes, J. A., Christensen, J. P., Devol, A. H., Naqvi, S. W. A., Paerl, H.
694 W., and Yoshinary, T.: The oceanic fixed nitrogen and nitrous oxide budgets: Moving targets
695 as we enter the anthropocene? Scientia Marina, 65, 85–105, 2001.

696 Cohen, A. S., O'Nions, R. K., Siegenthaler, R., and Griffin, W. L.: Chronology of the
697 pressure-temperature history recorded by a granulite terrain, Contributions to Mineralogy and
698 Petrology, 98, 303–311, 1988.

699 Conroy, J. L., Restrepo, A., Overpeck, J. T., Steinitz-Kannan, M., Cole, J. E., Bush, M. B.,
700 and Colinvaux, P. A.: Unprecedented recent warming of surface temperatures in the eastern
701 tropical Pacific Ocean, Nature Geoscience, 2, 46–50, 2008. doi:10.1038/ngeo390

702 Dalsgaard, T., Canfield, D. E., Petersen, J., Thamdrup, B., and Acuna-González, J.: N2
703 production by the anammox reaction in the anoxic water column of Golfo Dulce, Costa Rica,
704 Nature, 422, 606–608, 2003.

705 De La Rocha, C. L., Brzezinski, M. A., and DeNiro, M. J.: Fractionation of silicon isotopes
706 by marine diatoms during biogenic silica formation, Geochimica et Cosmochimica Acta,
707 61(23), 5051–5056, 1997.

De La Rocha, C. L., Brzezinski, M. A., DeNiro, M. J., and Shemesh, A.: Silicon-isotope composition of diatoms as an indicator of past oceanic changes, Nature, 395, 680–683, 1998.

De Pol-Holz, R., Robinson, R. S., Hebbeln, D., Sigman, D. M., and Ulloa, O.: Controls on sedimentary nitrogen isotopes along the Chile margin, Deep-Sea Research II, 56, 1042–1054, 2009. doi:10.1016/j.dsr2.2008.09.014

De Pol-Holz, R., Ulloa, O., Dezileau, L., Kaiser, J., Lamy, F., and Hebbeln, D.: Melting of the Patagonian Ice Sheet and deglacial perturbations of the nitrogen cycle in the eastern South Pacific, Geophysical Research Letters, 33(L04704), 2006. doi:10.1029/2005GL024477

De Pol-Holz, R., Ulloa, O., Lamy, F., Dezileau, L., Sabatier, P., and Hebbeln, D.: Late Quaternary variability of sedimentary nitrogen isotopes in the eastern South Pacific Ocean, Paleoceanography, 22(PA2207), 2007. doi:10.1029/2006PA001308

De Souza, G. F., Reynolds, B. C., Rickli, J., Frank, M., Saito, M. A., Gerringa, L. J. A., and Bourdon, B.: Southern Ocean control of silicon stable isotope distribution in the deep Atlantic Ocean, Global Biogeochemical Cycles, 26(GB2035), 2012. doi:10.1029/2011GB004141

DeMaster, D. J.: The supply and accumulation of silica in the marine environment, Geochimica et Cosmochimica Acta, 45, 1715–1732, 1981.

DeNiro, M. J., and Epstein, S.: Influence of diet on the distribution of nitrogen isotopes in animals, Geochimica et Cosmochimica Acta, 45(3), 341–351, 1981.

Díaz-Ochoa, J. A., Lange, C. B., Pantoja, S., De Lange, G. J., Gutiérrez, D., Munoz, P., and Salamanca, M.: Fish scales in sediments from off Callao, central Peru, Deep-Sea Research II, 56, 1113–1124, 2009. doi:10.1016/j.dsr2.2008.09.015

Díaz-Ochoa, J. A., Pantoja, S., De Lange, G. J., Lange, C. B., Sánchez, G. E., Acuña, V. R., Muñoz, P., and Vargas, G.: Oxygenation variability in Mejillones Bay, off northern Chile, during the last two centuries, Biogeosciences, 8(1), 137–146, 2011. doi:10.5194/bg-8-137-2011

733 Egan, K. E., Rickaby, R. E. M., Leng, M. J., Hendry, K. R., Sloane, H. J., Bostock, H. C., and
734 Halliday, A. N.: Diatom silicon isotopes as a proxy for silicic acid utilisation: A Southern
735 Ocean core top calibration, Geochimica et Cosmochimica Acta, 96, 174–192, 2012.
736 doi:10.1016/j.gca.2012.08.002

737 Ehlert, C., Grasse, P., Mollier-Vogel, E., Böschen, T., Franz, J., De Souza, G. F., Reynolds,
738 B. C., Stramma, L., and Frank, M.: Factors controlling the silicon isotope distribution in
739 waters and surface sediments of the Peruvian coastal upwelling, Geochimica et
740 Cosmochimica Acta, 99, 128–145, 2012. doi:10.1016/j.gca.2012.09.038

741 Ehlert, C., Grasse, P., and Frank, M.: Changes in silicate utilisation and upwelling intensity
742 off Peru since the Last Glacial Maximum - insights from silicon and neodymium isotopes,
743 Quaternary Science Reviews, 72, 18–35, 2013. doi:10.1016/j.quascirev.2013.04.013

744 Estrada, M., and Blasco, D.: Phytoplankton assemblages in coastal upwelling areas, In: C.
745 Bas, R. Margalef, and P. Rubies (Eds.), Simposio Internacional Sobre Las Areas de
746 Afloramiento Mas Importantes del Oeste Africano (Cabo Blanco y Benguela), Barcelona:
747 Instituto de Investigaciones Pesqueras, 379–402. 1985.

748 Georg, R. B., Reynolds, B. C., Frank, M., and Halliday, A. N.: New sample preparation
749 techniques for the determination of Si isotopic compositions using MC-ICPMS, Chemical
750 Geology, 235, 95–104, 2006. doi:10.1016/j.chemgeo.2006.06.006

751 Goldstein, S. L., O'Nions, R. K., & Hamilton, P. J.: A Sm - N d isotopic study of atmospheric
752 dusts and particulates from major river systems, Earth and Planetary Science Letters, 70(2),
753 221–236, 1984.

754 Grasse, P., Stichel, T., Stumpf, R., Stramma, L., and Frank, M.: The distribution of
755 neodymium isotopes and concentrations in the Eastern Equatorial Pacific: Water mass
756 advection versus particle exchange, Earth and Planetary Science Letters, 353-354, 198–207,
757 2012. doi:10.1016/j.epsl.2012.07.044

758 Grasse, P., Ehlert, C., and Frank, M.: The Influence of Water Mass Mixing on the Dissolved
759 Si Isotope Composition in the Eastern Equatorial Pacific, Earth and Planetary Science Letters,
760 380, 60–71, 2013. doi:10.1016/j.epsl.2013.07.033

761 Grousset, F. E., Biscaye, P. E., Zindler, A., Prospero, J., and Chester, R.: Neodymium
762 isotopes as tracers in marine sediments and aerosols: North Atlantic, Earth and Planetary
763 Science Letters, 87, 367–378, 1988.

764 Grove, M. J.: The initiation of the "Little Ice Age" in regions round the North Atlantic,
765 Climatic Change, 48, 53–82, 2001.

766 Gutiérrez, D., Sifeddine, A., Field, D. B., Ortlieb, L., Vargas, G., Chavez, F. P., Velazco, F.,
767 Ferreira-Bartrina, V., Tapia, P. M., Salvatteci, R., Boucher, H., Morales, M. C., Valdés, J.,
768 Reyss, J.-L., Campusano, A., Boussafir, M., Mandeng-Yogo, M., García, M., and
769 Baumgartner, T.: Rapid reorganization in ocean biogeochemistry off Peru towards the end of
770 the Little Ice Age, Biogeosciences, 6, 835–848, 2009.

771 Gutiérrez, D., Sifeddine, A., Reyss, J.-L., Vargas, G., Velazco, F., Salvatteci, R., Ferreira-
772 Bartrina, V., Ortlieb, L., Field, D. B., Baumgartner, T., Boussafir, M., Boucher, H., Valdés, J.,
773 Marinovic, L., Soler, P., and Tapia, P. M.: Anoxic sediments off Central Peru record
774 interannual to multidecadal changes of climate and upwelling ecosystem during the last two
775 centuries, Advances in Geosciences, 6, 119–125, 2006.

776 Horn, M. G., Robinson, R. S., Rynearson, T. A., and Sigman, D. M.: Nitrogen isotopic
777 relationship between diatom-bound and bulk organic matter of cultured polar diatoms,
778 Paleoceanography, 26(PA3208), 2011. doi:10.1029/2010PA002080

779 Horwitz, E. P., Chiarizia, R., and Dietz, M. L.: A Novel Strontium-Selective Extraction
780 Chromatographic Resin, Solvent Extraction and Ion Exchange, 10(2), 313–336, 1992.
781 doi:10.1080/07366299208918107

782 Hutchins, D. A., Hare, C. E., Weaver, R. S., Zhang, Y., Firme, G. F., DiTullio, G. R., Alm,
783 M. B., Riseman, S. F., Maucher, J. M., Geesey, M. E., Trick, C. G., Smith, G. J., Rue, E. L.,
784 Conn, J., and Bruland, K. W.: Phytoplankton iron limitation in the Humboldt Current and
785 Peru Upwelling, Limnology and Oceanography, 47(4), 997–1011, 2002.

786 Kanner, L. C., Burns, S. J., Cheng, H., Edwards, R. L., and Vuille, M.: High-resolution
787 variability of the South American summer monsoon over the last seven millennia: insights

from a speleothem record from the central Peruvian Andes. Quaternary Science Reviews, 75, 1–10, 2013. doi:10.1016/j.quascirev.2013.05.008

Kessler, W. S.: The circulation of the eastern tropical Pacific: A review, Progress in Oceanography, 69, 181–217, 2006. doi:10.1016/j.pocean.2006.03.009

Lacan, F., and Jeandel, C.: Tracing Papua New Guinea imprint on the central Equatorial Pacific Ocean using neodymium isotopic compositions and Rare Earth Element patterns, Earth and Planetary Science Letters, 186, 497–512, 2001.

Lam, P., Lavik, G., Jensen, M. M., Van de Vossenberg, J., Schmid, M., Woebken, D., Gutiérrez, D., Amann, R., Jetten, M. S. M., and Kuypers, M. M. M.: Revising the nitrogen cycle in the Peruvian oxygen minimum zone, PNAS, 106(12), 4752–4757, 2009.

Lamb, H. H.: The early Medieval Warm Epoch and its sequel, Palaeogeography, Palaeoclimatology, Palaeoecology, 1, 13–37, 1965.

Lamy, F., Hebbeln, D., Röhl, U., and Wefer, G.: Holocene rainfall variability in southern Chile: a marine record of latitudinal shifts of the Southern Westerlies. Earth and Planetary Science Letters, 185, 369–382, 2001.

Liu, K.-K., and Kaplan, I. R.: The eastern tropical Pacific as a source of 15N-enriched nitrate in seawater off southern Califomia. Limnology and Oceanography, 34(5), 820–830, 1989.

Mariotti, A., Germon, J. C., Hubert, P., Kaiser, P., Letolle, R., Tardieux, A., and Tardieux, P.: Experimental determination of nitrogen kinetic isotope fractionation: some principles; illustration for the denitrification and nitrification processes, Plant and Soil, 62, 413–430, 1981.

Meysman, F. J. R., Boudreau, B. P., and Middelburg, J. J.: Modeling reactive transport in sediments subject to bioturbation and compaction, Geochimica et Cosmochimica Acta, 69(14), 3601–3617, 2005. doi:10.1016/j.gca.2005.01.004

812 Minagawa, M., and Wada, E.: Stepwise enrichment of 15N along food chains: Further
813 evidence and the relation between d15N and animal age, Geochimica et Cosmochimica Acta,
814 48(5), 1135–1140, 1984.

815 Molina-Cruz, A.: The Relation of the Southern Trade Winds to Upwelling Processes during
816 the Last 75,000 Years, Quaternary Research, 8, 324–338, 1977.

817 Mollier-Vogel, E., Ryabenko, E., Martinez, P., Wallace, D. W. R., Altabet, M. A., and
818 Schneider, R. R.: Nitrogen isotope gradients off Peru and Ecuador related to upwelling,
819 productivity, nutrient uptake and oxygen deficiency, Deep-Sea Research I, 70, 14–25, 2012.
820 doi:10.1016/j.dsr.2012.06.003

821 Montes, I., Schneider, W., Colas, F., Blanke, B., and Echevin, V.: Subsurface connections in
822 the eastern tropical Pacific during La Niña 1999 – 2001 and El Niño 2002 – 2003, Journal of
823 Geophysical Research, 116(C12022), 2011. doi:10.1029/2011JC007624

824 Morley, D. W., Leng, M. J., Mackay, A. W., Sloane, H. J., Rioual, P., and Battarbee, R. W.:
825 Cleaning of lake sediment samples for diatom oxygen isotope analysis, Journal of
826 Paleilimnology, 31, 391–401, 2004.

827 Müller, P. J., and Schneider, R. R.: An automated leaching method for the determination of
828 opal in sediments and particulate matter, Deep-Sea Research I, 40(3), 425–444, 1993.

829 Piepgras, D. J., and Wasserburg, G. J.: Isotopic Composition of Neodymium in Waters from
830 the Drake Passage, Science, 217, 207–214, 1982.

831 Rabatel, A., Francou, B., Jomelli, V., Naveau, P., and Grancher, D.: A chronology of the
832 Little Ice Age in the tropical Andes of Bolivia (16°S) and its implications for climate
833 reconstruction, Quaternary Research, 70(2), 198–212, 2008. doi:10.1016/j.yqres.2008.02.012

834 Reuter, J., Stott, L., Khider, D., Sinha, A., Cheng, H., and Edwards, R. L.: A new perspective
835 on the hydroclimate variability in northern South America during the Little Ice Age,
836 Geophysical Research Letters, 36(L21706), 2009. doi:10.1029/2009GL041051

Reynolds, B. C., Aggarwal, J., André, L., Baxter, D. C., Beucher, C. P., Brzezinski, M. A., Engström, E., Georg, R. B., Land, M., Leng, M. J., Opfergelt, S., Rodushkin, I., Sloane, H. J., Van den Boorn, S. H. J. M., Vroon, P. Z., and Cardinal, D.: An inter-laboratory comparison of Si isotope reference materials, Journal of Analytical Atomic Spectrometry, 22(5), 561, 2007. doi:10.1039/b616755a

Reynolds, B. C., Frank, M., and Halliday, A. N.: Evidence for a major change in silicon cycling in the subarctic North Pacific at 2.73 Ma, Paleoceanography, 23(PA4219), 2008. doi:10.1029/2007PA001563

Sachs, J. P., Sachse, D., Smittenberg, R. H., Zhang, Z., Battisti, D. S., and Golubic, S.: Southward movement of the Pacific intertropical convergence zone AD 1400-1850, Nature Geoscience, 2, 519–525, 2009. doi:10.1038/NGEO554

Salvatteci, R., Gutiérrez, D., Field, D. B., Sifeddine, A., Ortlieb, L., Bouloubassi, I., Boussafir, M., Boucher, H., and Cetin, F.: The response of the Peruvian Upwelling Ecosystem to centennial-scale global change during the last two millennia, Climate of the Past, 10(2), 715-731, 2014a. doi: 10.5194/cp-10-715-2014

Salvatteci, R., Field, D. B., Sifeddine, A., Ortlieb, L., Ferreira-Bartrina, V., Baumgartner, T., Caquineau, S., Velazco, F., Reyss, J.-L., Sanchez-Cabeza, J. A., and Gutiérrez, D.: Cross-stratigraphies from a seismically active mud lens off Peru indicate horizontal extensions of laminae, missing sequences, and a need for multiple cores for high resolution records, Marine Geology, 357, 72-89, 2014b. doi: 10.1016/j.margeo.2014.07.008

Sarbas, B., and Nohl, U.: The GEOROC database – A decade of "online geochemistry", Geochimica et Cosmochimica Acta, (Goldschmidt Abstracts), A1158, 2009.

Scheidegger, K. F., and Krissek, L. A.: Dispersal and deposition of eolian and fluvial sediments off Peru and northern Chile, Geological Society of America Bulletin, 93(2), 150–162, 1982. doi:10.1130/0016-7606(1982)93<150

Sifeddine, A., Gutiérrez, D., Ortlieb, L., Boucher, H., Velazco, F., Field, D. B., Vargas, G., Boussafir, M., Salvatteci, R., Ferreira-Bartrina, V., García, M., Valdés, J., Caquineau, S., Mandeng-Yogo, M., Cetin, F., Solis, J., Soler, P., and Baumgartner, T.: Laminated sediments

865 from the central Peruvian continental slope: A 500 year record of upwelling system
866 productivity, terrestrial runoff and redox conditions, Progress in Oceanography, 79, 190–197,
867 2008. doi:10.1016/j.pocean.2008.10.024

868 Sutton, J. N., Varela, D. E., Brzezinski, M. A., and Beucher, C. P.: Species-dependent silicon
869 isotope fractionation by marine diatoms, Geochimica et Cosmochimica Acta, 104, 300–309,
870 2013. doi:10.1016/j.gca.2012.10.057

871 Takeda, S.: Influence of iron availability on nutrient consumption ratio of diatoms in oceanic
872 waters, Nature, 393, 774–777, 1998.

873 Tanaka, T., Togashi, S., Kamioka, H., Amakawa, H., Kagami, H., Hamamoto, T., Yuhara,
874 M., Orihashi, Y., Yoneda, S., Shimizu, H., Kunimaru, T., Takahashi, K., Yanagi, T., Nakano,
875 T., Fujimaki, H., Shinjo, R., Asahara, Y., Tanimizu, M., and Dragusanu, C.: JNdi-1: a
876 neodymium isotopic reference in consistency with LaJolla neodymium, Chemical Geology,
877 168, 279–281, 2000.

878 Unkel, I., Kadereit, A., Mächtle, B., Eitel, B., Kromer, B., Wagner, G., and Wackler, L.:
879 Dating methods and geomorphic evidence of palaeoenvironmental changes at the eastern
880 margin of the South Peruvian coastal desert (14°30'S) before and during the Little Ice Age,
881 Quaternary International, 175, 3–28, 2007. doi:10.1016/j.quaint.2007.03.006

882 Valdés, J., Ortlieb, L., Gutiérrez, D., Marinovic, L., Vargas, G., and Sifeddine, A.: 250 years
883 of sardine and anchovy scale deposition record in Mejillones Bay, northern Chile, Progress in
884 Oceanography, 79(2-4), 198–207, 2008. doi:10.1016/j.pocean.2008.10.002

885 Vargas, G., Pantoja, S., Rutllant, J. A., Lange, C. B., and Ortlieb, L.: Enhancement of coastal
886 upwelling and interdecadal ENSO-like variability in the Peru-Chile Current since late 19th
887 century, Geophysical Research Letters, 34(L13607), 2007. doi:10.1029/2006GL028812

888 Vuille, M., Francou, B., Wagnon, P., Juen, I., Kaser, G., Mark, B. G., and Bradley, R. S.:
889 Climate change and tropical Andean glaciers: Past, present and future, Earth-Science
890 Reviews, 89, 79–96, 2008. doi:10.1016/j.earscirev.2008.04.002

891 Wada, E., and Hattori, A.: Nitrogen isotope effects in the assimilation of inorganic
892 nitrogenous compounds by marine diatoms, Geomicrobiology Journal, 1(1), 85–101, 1978.
893 doi:10.1080/01490457809377725

894

Table 1. Downcore records of core M77/1-470 for $\delta^{30}Si_{opal}$ (‰), bSi content (wt%) and $^{143}Nd/^{144}Nd$, ε_{Nd} and $^{87}Sr/^{86}Sr$ of detrital material. $2\sigma_{(sd)}$ represents the external reproducibilities of repeated sample (Si) and standard (Nd, Sr) measurements.

depth (cm)	$\delta^{30}Si_{opal}$ (‰)	$2\sigma_{(sd)}$	bSi (wt%)	$^{143}Nd/^{144}Nd_{detritus}$	$\varepsilon_{Nd\ detritus}$	$2\sigma_{(sd)}$	$^{87}Sr/^{86}Sr_{detritus}$	$2\sigma_{(sd)}$
0.5	1.03	0.15	18.8	-	-	-	-	-
1.5	-	-	18.6	-	-	-	-	-
2.5	-	-	22.2	-	-	-	-	-
3.5	0.93	0.08	16.9	0.512369	-5.2	0.3	0.709315	1.5E-05
4.5	-	-	16.3	-	-	-	-	-
5.5	-	-	17.2	0.512381	-5.0	0.3	0.709356	1.5E-05
7	-	-	19.5	-	-	-	-	-
9	0.96	0.09	19.8	0.512398	-4.7	0.3	0.708822	1.5E-05
11	-	-	18.8	-	-	-	-	-
13	-	-	15.9	-	-	-	-	-
15	-	-	-	0.512383	-5.0	0.3	0.708737	1.5E-05
16	0.96	0.07	19.3	-	-	-	-	-
19	-	-	-	0.512386	-4.9	0.3	0.708552	1.5E-05
20	1.05	0.10	18.9	0.512410	-4.5	0.3	0.708412	8.0E-06
23	-	-	-	0.512393	-4.8	0.3	0.708720	1.5E-05
24	1.15	0.13	26.9	-	-	-	-	-
26	-	-	-	0.512387	-4.9	0.3	0.707482	8.0E-06
27	-	-	-	0.512397	-4.7	0.3	0.707555	1.5E-05
28	1.00	0.14	14.0	-	-	-	-	-
29	-	-	-	0.512452	-3.6	0.3	0.706549	1.5E-05
32	0.55	0.17	10.1	0.512442	-3.8	0.3	0.706763	1.5E-05
32	-	-	-	0.512445	-3.8	0.3	0.706469	8.0E-06
36	1.10	0.15	14.4	0.512419	-4.3	0.3	0.706767	8.0E-06
40	0.79	0.11	12.3	0.512408	-4.5	0.3	0.706964	8.0E-06
44	0.91	0.18	15.0	0.512421	-4.2	0.3	0.707057	8.0E-06
48	0.75	0.05	-	0.512395	-4.7	0.3	0.707816	8.0E-06

900 Table 2. Downcore records of core B0405-6 for $\delta^{30}Si_{opal}$ (‰), $bSiO_2$ content (wt%) and
901 $^{143}Nd/^{144}Nd$, ε_{Nd} and $^{87}Sr/^{86}Sr$ of detrital material. $2\sigma_{(sd)}$ represents the external
902 reproducibilities of repeated sample (Si) and standard (Nd, Sr) measurements.

year AD	$\delta^{30}Si_{opal}$ (‰)	$2\sigma_{(sd)}$	bSi (wt%)	$^{143}Nd/^{144}Nd_{detritus}$	$\varepsilon_{Nd\ detritus}$	$2\sigma_{(sd)}$	$^{87}Sr/^{86}Sr_{detritus}$	$2\sigma_{(sd)}$
1950	0.91	0.15	21.7	0.512507	-2.6	0.1	0.708372	8.0E-06
1925	0.83	0.15	21.0	0.512460	-3.5	0.3	0.707923	8.0E-06
1903	0.62	0.10	18.9	0.512487	-2.9	0.3	0.707715	8.0E-06
1857	1.02	0.16	34.4	0.512471	-3.3	0.3	0.707829	8.0E-06
1857	1.22	0.14	37.7	0.512481	-3.1	0.1	0.707736	8.0E-06
1818	0.56	0.15	12.6	0.512468	-3.3	0.3	0.707702	8.0E-06
1793	0.82	0.14	15.8	0.512446	-3.7	0.3	0.707265	8.0E-06
1761	0.71	0.16	13.5	0.512627	-0.2	0.3	0.707296	8.0E-06
1698	0.73	0.09	17.3	0.512462	-3.4	0.3	0.707278	8.0E-06
1564	0.81	0.12	20.8	0.512467	-3.3	0.3	0.707281	8.0E-06
1475	0.77	0.04	17.1	0.512427	-4.1	0.3	0.707959	8.0E-06
1370	0.80	0.23	34.2	0.512509	-2.5	0.3	0.707111	8.0E-06

903

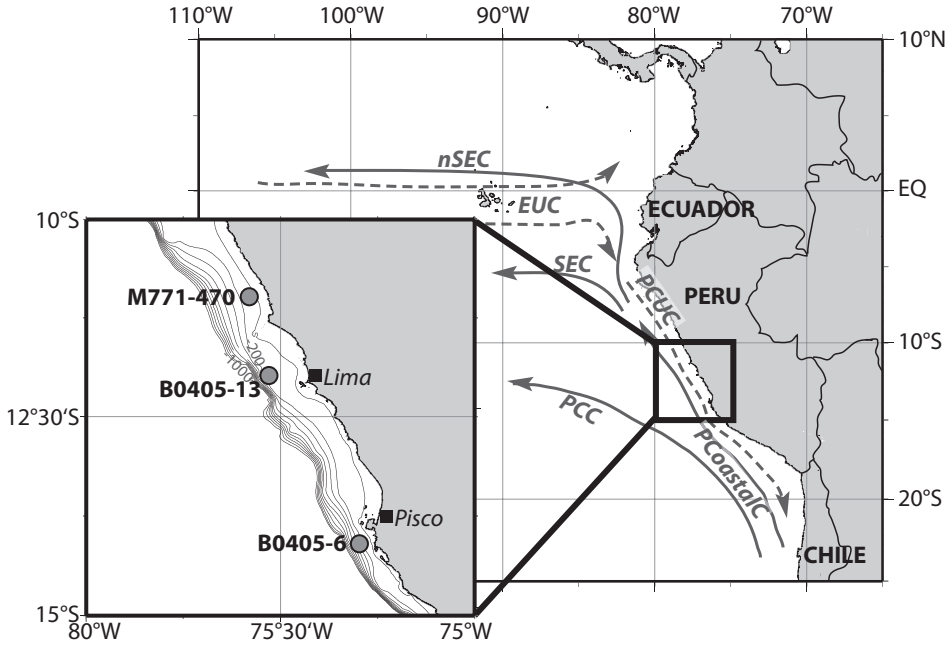

Figure 1. Schematic circulation patterns in the Eastern Equatorial Pacific. Surface currents (solid lines): (n)SEC: (northern) South Equatorial Current, PCC: Peru-Chile Current, PCoastalC: Peru Coastal Current; subsurface currents (dashed lines): EUC Equatorial Undercurrent, PCUC Peru-Chile Undercurrent (after Brink, 1983; Kessler, 2006), the inset shows the detailed location of cores M771-470, B0405-6 and B0405-13 (grey dots). The bathymetry is given for 0 to 1000 m water depth in 100 m increments.

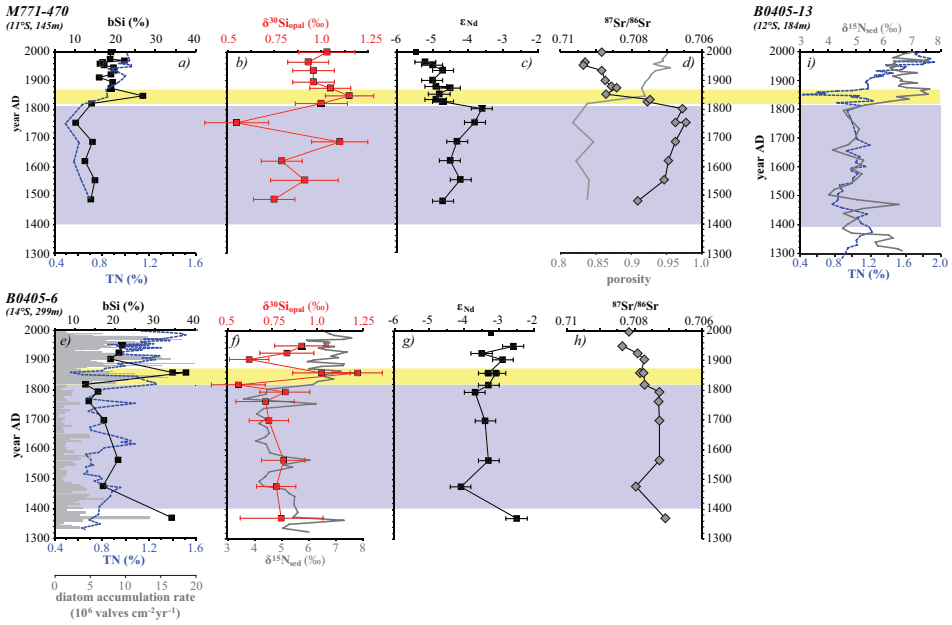

912

913 Figure 2. Downcore records for core M771-470 (upper panel) and core B0405-6 (lower
914 panel). The blue and yellow shadings indicate the age range of the LIA and the transitional
915 period, respectively. a/e) bSi concentration (black squares), total N concentration (dashed blue
916 curve), e) diatom accumulation rate (grey bars) (Gutiérrez et al., 2009), b/f) $\delta^{30}Si_{opal}$ (red
917 squares), f) bulk $\delta^{15}N_{sed}$ (grey curve) (Gutiérrez et al., 2009), c/g) $\varepsilon_{Nd\ detritus}$ (black squares),
918 d/h) $^{87}Sr/^{86}Sr_{detritus}$ (grey diamonds, x-axis is inverted), d) sediment porosity (grey curve).
919 Error bars represent $2\sigma_{(sd)}$ external reproducibilities of repeated standard or sample
920 measurements. Panel i) for comparison shows the total N content and $\delta^{15}N_{sed}$ of core B0405-
921 13 (Gutiérrez et al., 2009).

922

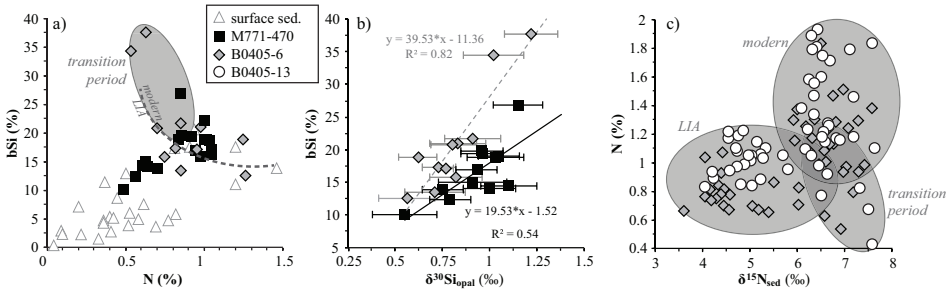

Figure 3. Surface sediment (white triangles) and downcore data (core M771-470: black squares, B0405-6: grey diamonds, B0405-13: white circles) for a) total N versus bSi concentrations (the dashed line marke the end of the LIA), b) $\delta^{30}Si_{opal}$ versus bSi concentration and c) $\delta^{15}N_{sed}$ versus total N concentrations. Error bars represent $2\sigma_{(sd)}$ external reproducibilities.

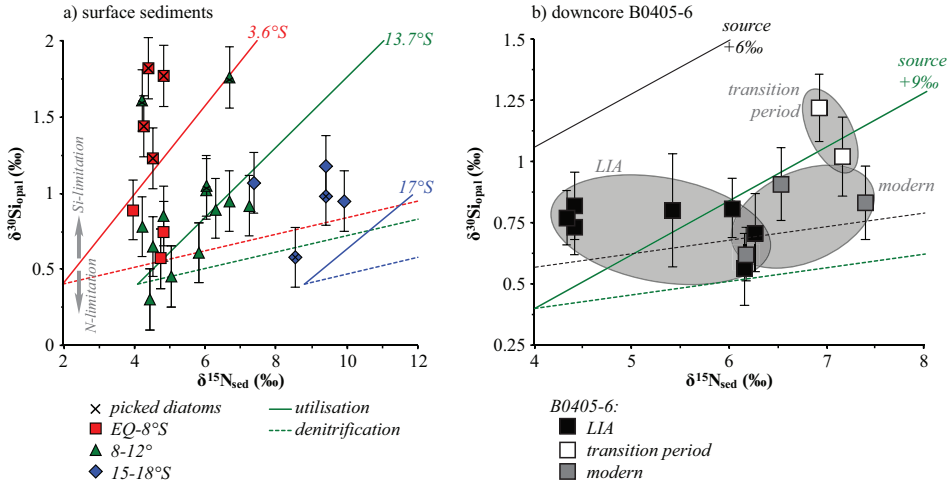

Figure 4. Relationship between $\delta^{15}N_{sed}$ versus $\delta^{30}Si_{opal}$ for a) surface sediments and b) downcore data from core B0405-6. The crosses in a) indicate $\delta^{30}Si$ data obtained from hand-picked diatoms, which reflect a different growth season than bulk $\delta^{30}Si_{opal}$ and which are influenced by stronger $Si(OH)_4$ limitation (higher $\delta^{30}Si$) (Ehlert et al., 2012). The solid lines reflect theoretical utilisation (assuming 1:1 utilisation of $Si(OH)_4$ and NO_3^- by the diatoms) and the dashed lines mark the theoretically expected line for denitrification, which represent the expected signal preserved in the sediments, based on present-day measurements: $\delta^{30}Si$ source signature and enrichment factor $\varepsilon_{diatom\text{-}Si(OH)4}$ are always +1.5‰ (Ehlert et al., 2012) and -1.1‰ (De La Rocha et al., 1997), respectively. $\delta^{15}N_{sed}$ source signature and $\varepsilon_{organic\text{-}NO3\text{-}}$ vary with latitude (Mollier-Vogel et al., 2012), in the north at 3.6°S source signature and ε are +5.7‰ and -3.7‰ (red curves), along the central shelf at 13.7°S source signature and ε are +8.9‰ and -4.8‰ (green curves), and in the south at 17°S source signature and ε were measured to be +14.5‰ and -5.7‰ (blue curves), respectively. The samples are colour-coded according to their location on the shelf and relative to the NO_3^- utilisation/NO_3^--loss that they experienced. Data points that plot above the utilisation curves reflect predominant $Si(OH)_4$ limitation whereas data points below record stronger NO_3^- limitation. The isotopic enrichment during denitrification was always set to be +20‰. For the downcore data (b) two different assumed source signatures are displayed: +9‰ (green lines, corresponding to the modern conditions along the central shelf region in a) and +6‰ (grey lines). Data points are colour-

coded according to the respective time periods (black: LIA, white: transition period, grey: modern). Error bars represent $2\sigma_{(sd)}$ external reproducibilities.

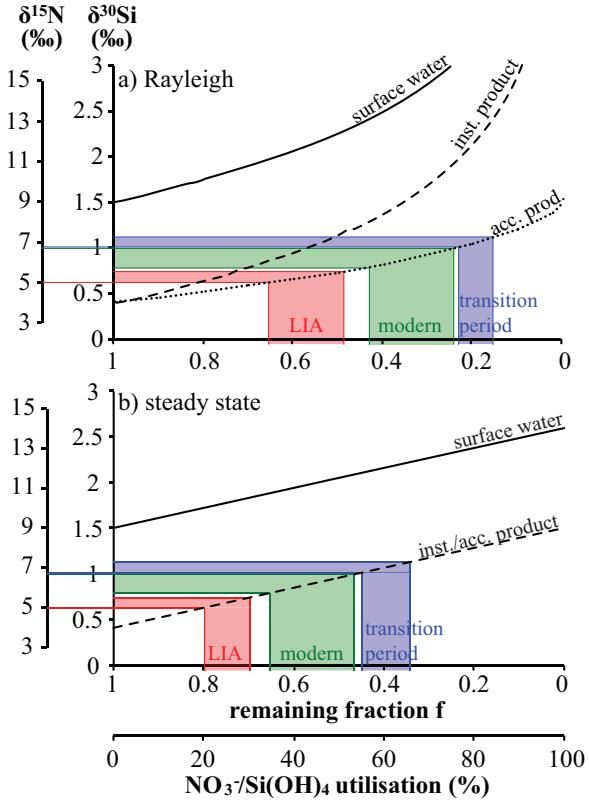

Figure 5. Theoretical changes in $\delta^{30}Si$ and $\delta^{15}N$ values of seawater and the instantaneous and accumulated product as a function of f (remaining nutrients from the available pool = [nutrient$_{observed}$]/[nutrient$_{initial}$]) with an initial $\delta^{30}Si_{Si(OH)4}$ value of +1.5‰ and $\delta^{15}N_{NO3-}$ of +9‰. The formation of the product, e.g. diatom opal, follows either a) Rayleigh-type fractionation or b) steady state-type fractionation behaviour, with enrichment factors ε of -1.1‰ ($\delta^{30}Si$) and -5‰ ($\delta^{15}N$) (corresponding to conditions along the modern central Peruvian shelf, see Fig. 4). The colour shadings mark the range of measured mean $\delta^{30}Si_{opal}$ (both cores) and $\delta^{15}N_{sed}$ (B0405-6 only) in the cores for the LIA (red), the transition period (blue) and modern sediments (green), from which the respective nutrient utilisation (%) can be deduced.

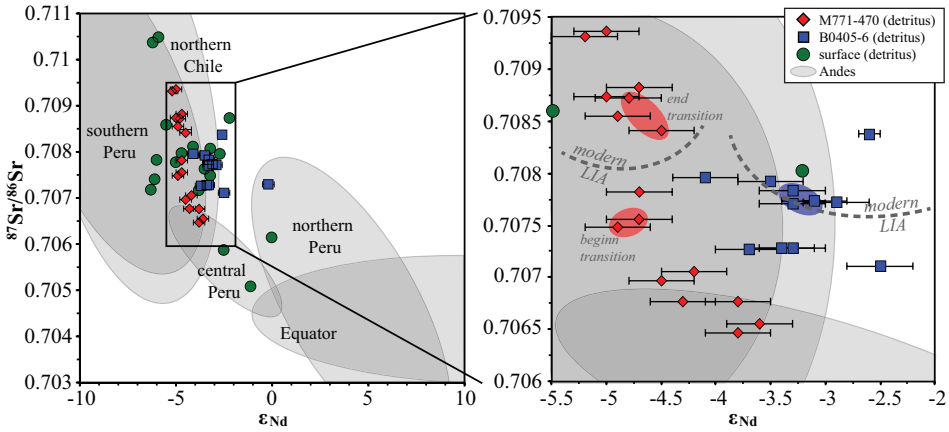

Figure 6. $\varepsilon_{Nd\ detritus}$ versus $^{87}Sr/^{86}Sr_{detritus}$ for core M771-470 (red diamonds) and B0405-6 (blue squares). Error bars represent $2\sigma_{(sd)}$ external reproducibilities. The green dots are data obtained from surface sediment samples at different sites on the Peruivian shelf. The grey shadings indicate potential sources and provenance endmembers of the detrital material.